

**MATERIAL FLOW STUDY DURING FRICTION STIR
WELDING OF DISSIMILAR MATERIAL**

by

KON KIT LUNG

DISSERTATION

Submitted to the Mechanical Engineering Programme
in Partial Fulfillment of the Requirements
for the Bachelor of Engineering (Hons)
(Mechanical Engineering)
MAY 2012

Universiti Teknologi PETRONAS
Bandar Seri Iskandar
31750 Tronoh
Perak Darul Ridzuan

Copyright
By
KON KIT LUNG, 2012

CERTIFICATION OF APPROVAL

CERTIFICATION OF ORIGINALITY

MATERIAL FLOW STUDY DURING FRICTION STIR WELDING OF DISSIMILAR MATERIAL

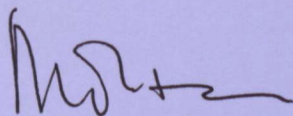
By

KON KIT LUNG

A project dissertation submitted to the
Mechanical Engineering Programme
Universiti Teknologi PETRONAS
in Partial Fulfillment of the Requirements
for the Bachelor of Engineering (Hons)
(Mechanical Engineering)

MAY 2012

Approved by,



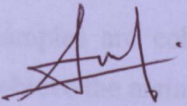
(Dr Mokhtar B Awang)

Universiti Teknologi PETRONAS
Bandar Seri Iskandar
31750 Tronoh
Perak Darul Ridzuan

ABSTRACT

CERTIFICATION OF ORIGINALITY

This is to certify that I am responsible for the work submitted in this project, that the original work is my own except as specified in the references and acknowledgements, and that the original work contained herein have not been undertaken or done by unspecified sources or persons



KON KIT LUNG

ACKNOWLEDGEMENTS

ABSTRACT

This research focuses on the material flow study of aluminium alloy 6092/SiC/25p metal matrix composite welded plate. In this research, friction stir welding is used as the joining method to join aluminium alloy 6061 and aluminium alloy 6092/SiC/25p metal matrix composite welded plate. Two different configurations are focused in this research. AA6061 plate is placed at advancing side and AA6092 MMC is placed at retreating side in configuration 1 and vice versa in configuration 2. First of all, suitable FSW tool with tapered angle is designed and fabricated following by determine the acceptable FSW parameters (feed rate and rotational speed) with least defects. FSW final run on both configurations are executed with acceptable parameters. Samples are collected from each configuration to be observed under optical microscope to achieve the main objective which is to study the material flow of silicon carbide in the weld zone in both configurations. The research has been successfully carried out and its findings showed that configuration 2 where AA6092 MMC is placed at advancing side has better FSW result with less wear at surface and minimal weld hole spotted. Apart from that, there is more SiC particles circulation from advancing to retreating side in configuration 2. This finding is proven by micro-hardness testing which showed that configuration 2 has average higher HV value as compared to configuration 1 and the zone with more SiC particles gave higher HV value.

ACKNOWLEDGEMENTS

I would like to take this opportunity to briefly recognize and express my appreciation and thankful the group of people and agencies which have assisted me with my final year project for the past 2 semesters which is approximately nine months. Firstly, I would like to express my high appreciation to my FYP supervisor, Dr Mokhtar B Awang for continuous advice and guidance to me throughout the whole project. Dr Mokhtar has been giving professional and useful recommendations to improve my FYP from time to time. Apart from that, lab technicians from mechanical department block 21, Mr Jani and Mr Saiful, have been very helpful in guiding me how to fabricate FSW tool using CNC lathe machine and operating of CNC Milling machine for FSW trial run and final run. Furthermore, Mr Zamil, expert in EDM wire cutting technique, is always helpful to provide proper cutting on the work pieces. Apart from that, Mr Mahfuzrazi, lab technician from block 17 has been very patient and kind in guiding me for FSW tool heat treatment and preparation of samples under Optical Microscope analysis. Last but not least, I would like to thank my family for supporting me in my FYP, senior and friend who have been helping and supporting me all the time.

TABLE OF CONTENTS

CERTIFICATION OF APPROVAL-----	i
CERTIFICATION OF ORIGINALTY-----	ii
ABSTRACT-----	iii
ACKNOWLEDGEMENTS-----	iv
TABLE OF CONTENT-----	v
LIST OF FIGURE-----	vii
LIST OF TABLE-----	x
CHAPTER 1: INTRODUCTION	
1.1 Project Background-----	1
1.2 Problem Statements-----	3
1.3 Objectives -----	3
1.4 Scope of Study-----	4
CHAPTER 2: LITERATURE REVIEW/THEORY-----5	
CHAPTER 3: METHODOLOGY	
3.1 Flow Chart/Process Flow-----	15
3.2 Friction Stir Welding Tool-----	16
3.2.1 Design of Welding Tool-----	16
3.2.2 Selection of Welding Tool Material-----	18
3.2.3 Fabrication & Heat Treatment of Welding Tool-----	19
3.3 EDM Wire Cutting of Workpieces -----	21
3.4 Friction Stir Welding Clamping System-----	21
3.5 Friction Stir Welding Joining Process-----	22
3.6 Sample Preparation for Analysis under Optical Microscope-----	23
CHAPTER 4: RESULTS AND DISCUSSIONS-----25	
4.1 FSW Trial Run & Preliminary Result-----	25

4.2 FSW Final Run -----	28
4.3 Configuration 1-----	29
4.4 Configuration 2-----	34
4.5 Micro-hardness Testing Along the Weld Zone For Both Configurations-----	39
4.6 Comparison and Discussion between Both Configurations-----	40
4.7 Analysis and Discussion on FSW Tool-----	40
CHAPTER 5: CONCLUSION & RECOMMENDATIONS-----	42
5.1 Conclusion -----	42
5.2 Recommendations -----	42
REFERENCES-----	43
APPENDIXES-----	44

LIST OF FIGURE

Figure 1: Schematic drawing of friction stir welding-----	1
Figure 2: Illustration of FSW process-----	1
Figure 3: Macrograph and micrograph of nugget zone of FSW on Al-4.5 Mg-0.26 Sc -----	6
Figure 4: Micro photography of based material -----	7
Figure 5: Micro photography of nugget -----	7
Figure 6: Micro photography of transition zone -----	7
Figure 7: FSW on AA 6061/SiC/17.5p -----	8
Figure 8: FSW using H-13 steel welding tool with 11ipm and variable rpm-----	8
Figure 9: FSW using CBN welding tool with different parameters -----	9
Figure 10: Tensile Failure locations of H13 tool and CBN Tool-----	9
Figure 11: SiC particulate distribution in the welds -----	10
Figure 12: Friction stir welding on aluminum alloy 6092 SiC 25p t6 metal matrix composite --	11
Figure 13: A typical onion flow of the FSW cross sectioned sample -----	11
Figure 14: Microstructure evaluations for friction stir in each different region are compared: (a) parent metal (b) HZAC region (c) TMAZ (d) centre of weld regions -----	12
Figure 15: FSW on AA5083H111-AA6351-----	12
Figure 16: Microstructures view: (a) Composed of different regions (b) TMAZ and FSP (c) Upper portion mixing of two Al alloys (d) Alternative lamellae (e) Upper portion of TMAZ in retreating side (f) Parent material of AA6351 (g) Parent material of AA5083-H111-----	13
Figure 17: Weld zone -----	14
Figure 18: FSW AUTOCAD drawings with dimension in unit of mm -----	17
Figure 19: H-13 steel-----	18

Figure 20: CNC lathe machine -----	19
Figure 21: CNC lathe coding and dimensions -----	19
Figure 22: Fabricated welding tool -----	19
Figure 23: Box furnace with control unit -----	20
Figure 24: Welding tools in the box furnace -----	20
Figure 25: Welding tool after heat treatment-----	20
Figure 26: AA 6061 plate after EDM wire cut -----	21
Figure 27: AA 6092/SIC 25p/T6 MMC after EDM wire cut -----	21
Figure 28: Sketch of customized clamping system with dimension-----	22
Figure 29: Fabricated clamping system-----	22
Figure 30: CNC milling machine: (a) Display panel board (b-d) FSW process -----	22
Figure 31: Preparation of OM samples: (a-b) Abrasive cutter (c) Mounting machine (d) Grinding process -----	23
Figure 32: Optical microscope-----	24
Figure 33: Micro-hardness testing machine-----	24
Figure 34: FSW trial run configuration-----	25
Figure 35: Result of FSW trial run surface -----	26
Figure 36: EDM wire cut on the welded plate-----	26
Figure 37: Welded plate of trial run after EDM cutting into 4 pieces-----	27
Figure 38: Tunnel defect at advancing side-----	27
Figure 39: FSW final run welded plates -----	28
Figure 40: Illustration of FSW final run configuration 1-----	29
Figure 41: FSW weld surface in configuration 1: (a) Splash at retreating side (b) Smooth weld surface-----	29

Figure 42: Defect hole in FSW configuration	30
Figure 43: Cross-section of configuration 1 from starting to ending	31
Figure 44: Cross-section in mountings A, B, C : (A) Beginning point (B) Middle point (C) Ending point	31
Figure 45: Parent material under OM 50X: (a) AA6061 (b) AA6092 MMC parent material under OM	32
Figure 46: SiC distribution line between nugget zone and TMAZ area at advancing side for 5X,10X and 50X under OM	32
Figure 47: SiC distribution: (a) Concentration of SiC at nugget zone (b) Transition Zone in Nugget Area	33
Figure 48: SiC distribution: (a) Unaffected zone in advancing side (b) HAZ & TMAZ areas at retreating side	33
Figure 49: Illustration of FSW final run configuration 2	34
Figure 50: Splash at retreating side at configuration 2	34
Figure 51: Silicon carbide particles at weld zone surface	35
Figure 52: Defect hole in FSW configuration 2	35
Figure 53: Cross-section of configuration 2 from starting to ending	36
Figure 54: Cross-section mountings D, E, F: (D) Beginning point (E) Middle point (F) Ending point	36
Figure 55: SiC distribution in configuration 2: (a) Clear SiC distribution line (b) Transition zone at weld nugget	37
Figure 56: SiC distribution (a) mixture of large and small SiC particles (b) large SiC particles at advancing side	37
Figure 57: Small SiC particles spotted at retreating side	38
Figure 58: Micro-hardness testing along weld zone for both configurations	39
Figure 59: FSW tool (a) before trial run (b) after trial run	41
Figure 60: FSW tool after final run	41

LIST OF TABLE

Table 1: Benefit classification of Friction Stir Welding-----	2
Table 2: FSW parameters for AL 6061/SiC/17.5p-----	7
Table 3: Comparison between H13 tool and CBN tool-----	10
Table 4: Palanivel's research welding parameters-----	13
Table 5: Design parameters of welding tool-----	16
Table 6: Chemical composition of H-13 steel-----	18
Table 7: FSW trial run parameters-----	25
Table 8: FSW final run parameters-----	28
Table 9: HV value of AA6061 and AA6092 MMC parent material-----	38

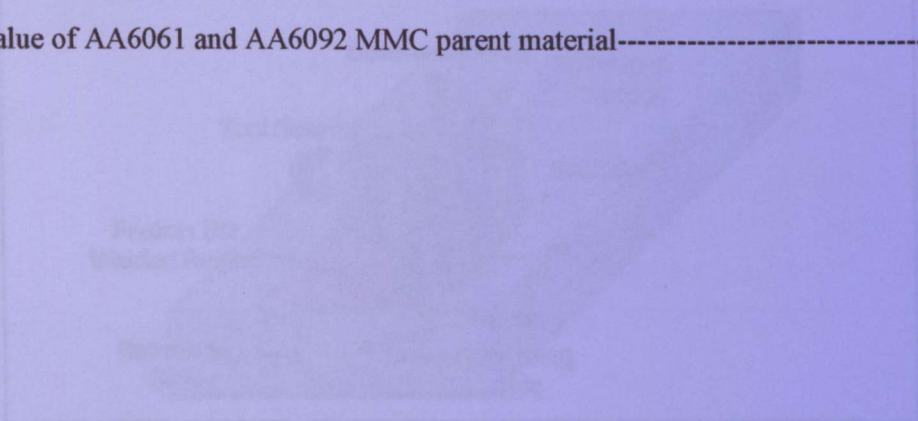


Figure 1: Schematic drawing of friction stir welding [3]



Figure 2: Illustration of FSW process [2]

FSW is treated as the most considerable development in joining metal in a decade and it is treated as "green" technology because of its energy efficiency, environment friendliness and versatility [3]. Compared to conventional welding methods, FSW uses significantly less energy as there is no cover gas or flux is used and thereby making the process environmentally friendly.

CHAPTER 1: INTRODUCTION

1.1 Project Background

Friction stir welding (FSW) was invented at The Welding Institute (TWI) of UK in year 1991 [1]. It is a solid-state joining method and it was at first applied to aluminum alloys. FSW is a mechanical, solid-state joining process which has been verified as a practicable joining method for many different joining configurations including lap joints, T joints, fillet joints and butt joints [2]. It is a simple concept when a non-consumable rotating welding tool with a unique designed pin and shoulder is inserted into abutting edges of two plates to be joined. Then, the tool will be traversed along joint line between the plates as displayed by figure 1. Figure 2 also illustrates FSW process.

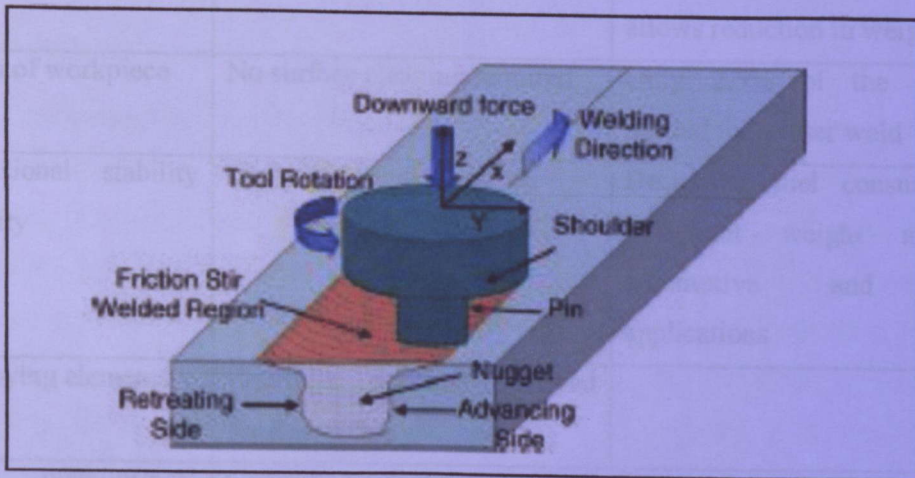


Figure 1: Schematic drawing of friction stir welding [3]

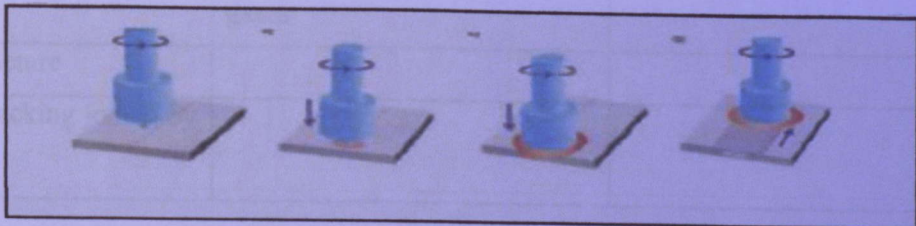


Figure 2: Illustration of FSW process [2]

FSW is treated as the most considerable development in joining metal in a decade and it is treated as “green” technology because of its energy efficiency, environment friendliness and versatility [3]. Compared to conventional welding methods, FSW uses significantly less energy as there is no cover gas or flux is used and thereby making the process environmentally friendly.

FSW joining does not involve the usage of filler metal to promote joining. Therefore, various aluminum alloy can be joined without occurring problem for the compatibility of composition, which brings issue in fusion welding.

Friction stir welding has several distinct advantages over traditional arc welding. FSW generates no fumes, results in reduced distortion and improved weld quality for the proper parameters, is adaptable to all positions, and is relatively quiet [3]. Benefit of FSW can be classified in table 1.

Table 1: Benefit classification of Friction Stir Welding [3]

Metallurgical Benefits	Environmental Benefits	Energy Benefits
Solid phase process	No shielding gas required	Improved materials use(e.g. joining different thickness) allows reduction in weight
Low distortion of workpiece	No surface cleaning required	Only 2.5% of the energy needed for a laser weld
Good dimensional stability and repeatability	Eliminate grinding wastes	Decreased fuel consumption in light weight aircraft, automotive and ship applications
No loss of alloying elements	Eliminate solvents required for degreasing	
Excellent metallurgical properties in the joint area	Consumable materials saving, such as rugs, wire or any other gases	
Fine microstructure		
Absence of cracking joined by fasteners		

However, FSW technology has some limitations. One of the limitations is the workpieces must be rigidly clamped before welding process is operated [2]. Apart from that, backing bar is required when self-reacting tool or directly opposed tool are not available. Furthermore, keyhole is occurred at ending point of each weld between the joint of two plates [1].

Nowadays, FSW is widely used to join aluminum alloys in marine and shipbuilding industries, aerospace, rail and automotive industry. Moreover, this technology contributes some significant advantages to aluminum extrusion industry. FSW has been used in automotive industries to fabricate suspensions arms and wheel rims. Aluminum panels are used to produce high speed ferries and panels for rail vehicles have applied FSW technique. Furthermore, application of FSW on 50mm thick copper material gives a possible solution to solve nuclear encapsulation of radioactive disposal. Friction stir welding is bringing success as a material joining technique and the prediction for the successful joining of various steel products looks promising.

Apart from that, metal matrix composite (MMC) is a new material in the industrial application. It has huge ability with its unique property with reinforced particles being imbedded in the matrix. Its application is utilized in both aerospace and automotive applications.

1.2 Problem Statement

Nowadays, FSW is a new welding technology which has been widely used in railway, aerospace and maritime industry. FSW is a mechanical, solid-state joining process which has been proven as a viable joining method. As the widely use of technology, there are lots of research being carried out to achieve further understanding and improvement on this technology. Although lots of researches are done, there are less attempts are done on metal matrix composite (MMCs). FSW on MMCs is new material with unique properties. Apart from that, limited research discussed FSW on dissimilar materials. The selected dissimilar materials in the research are MMC with aluminum alloy which are fresh combination and less research of FSW on these materials has been done. Apart from that, implementation of FSW on these materials is fresh in the industry and the successful of the research would benefit the industry application.

1.3 Objective

The main objective of the project is to study the SiC particles distribution at the weld zone by analyzing its micro-hardness and microstructures under optical microscope.

1.4 Scope of Study

This research focuses on dissimilar material which includes aluminum alloy 6092/SIC 25p/T6 MMC plate and aluminum alloy 6061 metal plate. There are four main parts in this research as below:

- I. To design and fabricate suitable friction stir welding tool for the research
- II. To obtain acceptable FSW parameters with minimal defects for the research
- III. To join Aluminum Alloy 6092/SIC 25p/T6 metal matrix composite plate and Aluminum Alloy 6061 plate successfully with minimal defects via two different configurations as below
 - a. Configuration 1
 - Advancing Side: Aluminum Alloy 6061 plate
 - Retreating Side: Aluminum Alloy 6092/SIC 25p/T6 metal matrix composite plate
 - b. Configuration 2
 - Advancing Side: Aluminum Alloy 6092/SIC 25p/T6 metal matrix composite plate
 - Retreating Side: Aluminum Alloy 6061 plate
- IV. To conduct and compare material flow study and micro-hardness test at the weld zone for each configuration

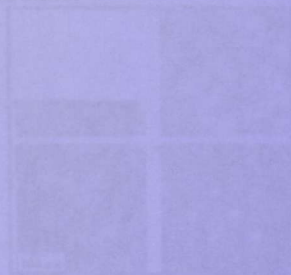


Figure 3: Micrograph and micrograph of nugget zone of FSW on Al-4.5Mg-0.26Sc [14]

CHAPTER 2: LITERATURE REVIEW/ THEORY

In this chapter, literature review were done based on previous friction stir welding research on aluminum alloy 6061, metal matrix composites, dissimilar materials and material flow of aluminum alloy. Additionally, we will review studies concerning FSW parameters to get the optimum weld zone. Special emphasis is placed on joining aluminum alloy series MMCs with pure aluminum alloy since the research is referring to FSW to join Aluminum Alloy 6092 SiC/20p with AA 6061.

Babu et al. [3] had conducted a research on FSW of AA6061 aluminum alloy. His research proved that the welded joint has higher tensile strength to weight ratio and finer micro structure. FSW of aluminum alloys has the ability to withhold great mechanical and metallurgical property. The tensile strength of AA6061 Aluminum alloy is discussed for optimum process parameters of rotational speed, welding speed and axial force. They stated that the optimum welding parameter of 1200rpm rotational speed, 75mm/min welding speed and 7KN axial force. They stressed that better tensile properties on weld joints were noticed as the result of formation of fine equiaxed grains and very fine strengthening precipitates is uniformly distributed in the weld region.

Apart from that, Munoz et al. [4] had conducted FSW on Al-4.5 Mg-0.26 Sc heat treated aluminum alloy. The centre of the friction stir weld was composed by the nugget and the flow arm, both exhibiting recrystallized equiaxed grains with a few microns in size. FSW nugget exhibited a fine recrystallized grains microstructure as well as fine-dispersed Al_3Sc hardening precipitates. Their size and shape as well as their distribution were not highly different than those observed in based material. Figure 3 shows the macrograph of FSW cross-section, TEM micrograph of the nugget zone, dark field of the nugget with Al_3Sc particles and diffraction pattern with superlattice Al_3Sc streaks.

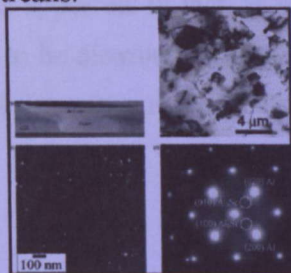


Figure 3: Macrograph and micrograph of nugget zone of FSW on Al-4.5 Mg-0.26 Sc [4]

They also stressed that the Mg content in nugget zone is the same as in based material and hence there is no inclusions rich in Mg are present.

Material flow of Aluminum alloy MMCs would have different pattern as compared to pure Aluminum Alloy. Marzoli et al.[5] had conducted friction stir welding research on metal matrix composite, AA6061, a precipitation hardenable aluminum alloy containing silicon and magnesium as major alloying elements, reinforced with 20% volume Al_2O_3 (alumina) particles. It was produced by Compo casting, then extruded into 7x100x1000mm plates and heat-treated to T6 temper condition. In their research, all welded plates were produced using the same tool, but with varies rotation speed. They stated that the FSW tool must be able to withstand the strong abrasion of the alumina particles during FSW process to avoid impurities in weld zone.

They also found out that a slower welding speed corresponds to a better heat input, which will generate a wider nugget in most of the cases. However, in the case of the MMCs, this occurrence was not as apparent as in the case of the unreinforced alloys as the reinforcement particles limited the flow of plasticized materials. The stirring and rotation of the tools had a substantial impact towards the distribution and shape of the reinforcement particles. It broke off sharp edges of larger particles and meanwhile rounding them up. The action resulted in plenty of small and round particles around the nugget. Material flow of aluminum matrix was partially hindered by the alumina particles, and the recrystallisation typical in the nugget of FSW alloys was not completed in this case. They proved that the presence of numerous small and round particles was observed in the Nugget zone, which was not present in parent material. This situation was explained by the stirring effect of the tool. It was high possibly due to the effect the tool's rotation which abrades the surface of the alumina particles. This phenomenon will cause the detachment of the pointed edges of the particles, thus creating the small particles and rounding up both the bigger ones. The distribution border line between the nugget and TMAZ was seen clearly. Small particles appeared, in fact, as soon as an influence of the stirring of the tool was detected and appeared to be distributed uniformly in the aluminum matrix. It is proved that the reinforcement particles behave on a macro scale like the grains in the base alloys.

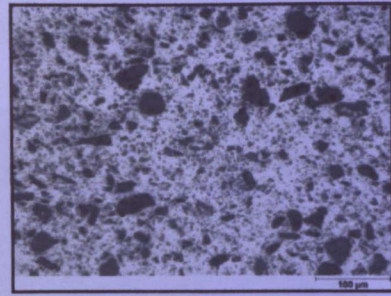
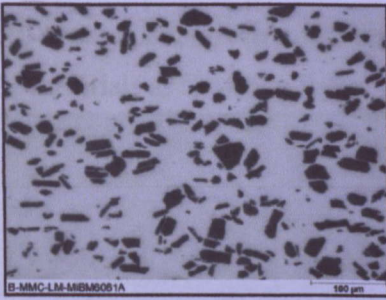


Figure 4: Micro photography of based material [5] Figure 5: Micro photography of nugget [5]

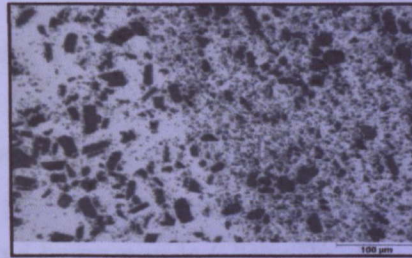


Figure 6: Micro photography of transition zone [5]

Another research on MMCs was conducted by Prater [6]. He had investigated on friction stir welding of AL 6061 and AL 6061/SiC/17.5p using diamond coatings tool welding. For aluminum MMC material, the considered rotation and traverse speed were lowered than weld matrix for unreinforced alloy, Al 6061. The optimum parameters of the FSW on AL 6061/SiC/17.5p were shown in table 2.

Table 2: FSW parameters for AL 6061/SiC/17.5p [6]

FSW Parameters	Value	Description
Travel Speed	10 mm/min	mm per minute horizontal speed
Rotating Speed	1350rpm	Rotating speed of pin tool
Lead Angle	2.5deg	Pin tool's tilting angle from vertical plane
Plunge depth	0.025 cm	Shoulder length plunges below crown side
Penetration Ligament	0.0125 cm	Distance between tip of pin and backing anvil

He proved that FSW on Al 6061/SiC/17.5p via butt joint produces a rougher texture surface than FSW on Al6061. The composite material was coarser in the pre-welded state than its

unreinforced counterpart, which might result for the difference in as-welded surface consistency between the materials as shown in figure 7.

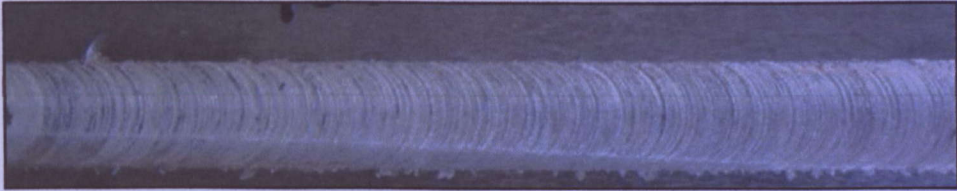


Figure 7: FSW on Al 6061/SiC/17.5p[6]

Moreover, Tracy et al. [7] had conducted the feasibility of joining AA 6092-17.5% SiC_p via FSW. In the research, Aluminum Alloy 6092-17.5% SiC_p with the dimension 0.1 inch thickness with 8 inch x 24 inch panels were used. The research found the best rotation speed and travel speed for the joining process of this material. The chosen tool materials were H13 tool steel and Polycrystalline cubic boron nitride (CBN). Welding parameters had been evaluated as rotation speed with 202, 545 and 815 rpm while traverse speed with 6.4, 11 and 26 ipm. Figure 8 shows FSW result with different parameters.

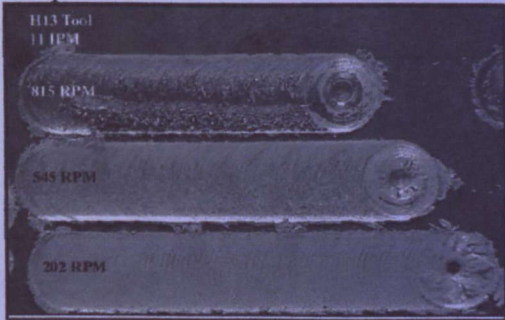


Figure 8: FSW using H-13 steel welding tool with 11IPM and variable RPM[7]

They said the optimum parameters for H-13 steel as welding tool were 545rpm rotational speed with 11ipm transverse speed. On other hand, welds made with CBN tooling produced no spalling of the surface, better consolidation and less flash. Figure 9 depicts the welds made by CBN welding tool [7].

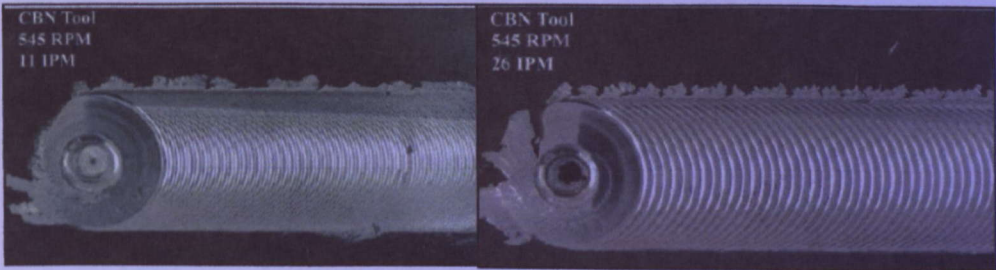


Figure 9: FSW using CBN welding tool with different parameters [7]

They stated that there were tensile failure locations on the weld zone. The findings proved that there were tensile failure locations at TMAZ and DXZ for H13 tool while there was only tensile failure at HAZ for CBN tool as shown in the figure 10.

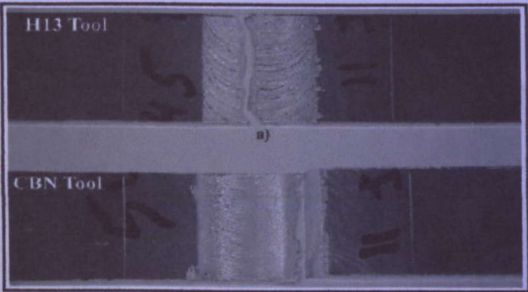


Figure 10: Tensile failure locations of H13 tool and CBN tool [7]

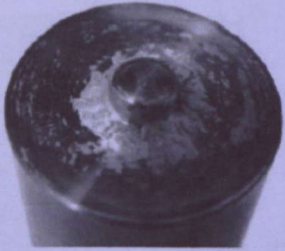

Apart from that, they also found out that the silicon carbides particulates distribution in the weld was same as in the base metal for both welding tool as illustrated in figure 11. Different welding tools had no effect on SiC particulates distribution.



Figure 11: SiC particulate distribution in the welds [7]

They concluded the tool wear between H-13 steel and CBN in table 3.

Table 3: Comparison between H13 tool and CBN Tool [7]

H13 tool after 6 feet of weld	CBN tool after 20 feet of weld
<ul style="list-style-type: none"> ➤ Loss on diameter of pin ➤ Loss of radius on shoulder ➤ Not feasible to produce significant length of weld  <p>H13 tool</p>	<ul style="list-style-type: none"> ➤ No measurable wear on any features  <p>CBN tool</p>

Friction stir welding on Aluminum alloy 6092 SiC 25p T6 metal matrix composite had been carried out by Umar et al. [5]. The selected dimension was 5 inches x 8 inches x 0.5inch with the material aged treated. The main objectives were to obtain its microstructure evolution and mechanical properties in weld zone. The selected welding tool is H13 tool steel. They kept the rotation speed of the FSW constant at 1200rpm while the traverse speed was kept at 8mm per minute. Figure 12 depicts the result of FSW in the research.

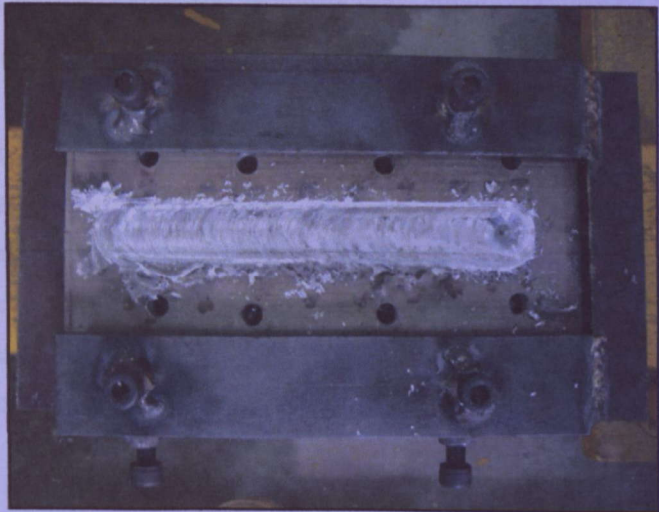


Figure 12: Friction stir welding on Aluminum alloy 6092 SiC 25p T6 metal matrix composite [8]

They proved that joining of the composite material through friction stir welding was successfully accomplished. Typical onion flow was obtained on these kinds of welds in figure 13 which were caused by the material flow during the joining process. It was also observed that there was minimal occurrence of splatter at the side of the welding line during the joining process. Upon the material sectioning, the two plates were welded perfectly without any visible defect with the selected welding tool and welding parameters.

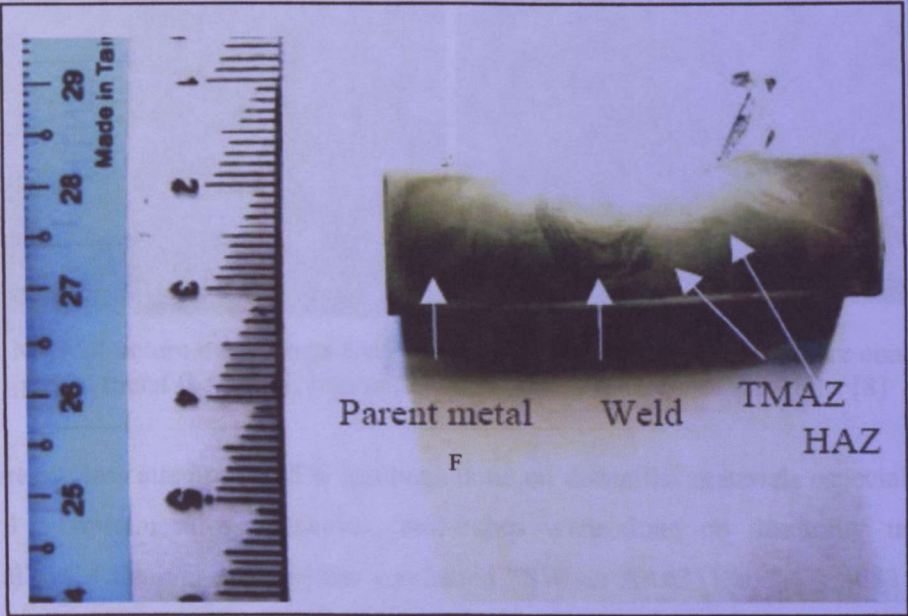


Figure 13: A typical onion flow of the FSW cross sectioned sample [8]

In the research, Scanning Electron Microscope (SEM) image had proved that there is no definite orientation of the SiC particulate in the base metal which is shown in the figure 14a. As compared to figure 14b, there was a significant case of particulate re-alignment. It was observed from the SEM micrograph that there was a definite concentration of SiC particulate in the TM-HAZ (figure 13b and figure 13c) region while there was a lesser concentration of the SiC particulate in the centre of the welding zone as shown in figure 13 d. The SEM imaging failed to show any breakage of the SiC particulate within the welding zone. It was observed from the SEM that there was no evidence of liquidation during the welding process when compared to fusion welding processes.

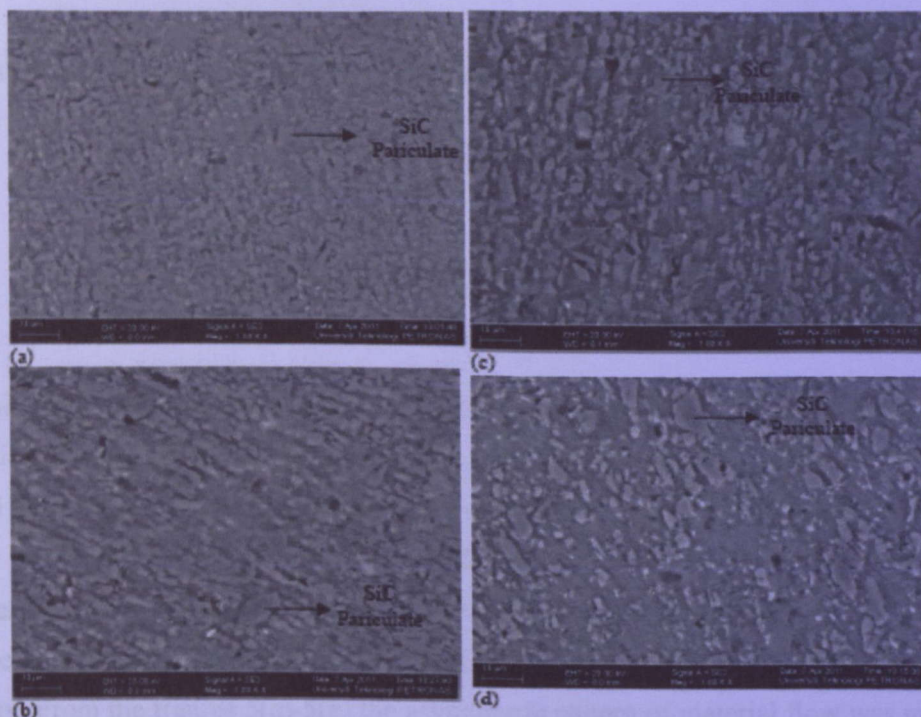


Figure 14: Microstructure evaluations for friction stir in each different region are compared: (a) parent metal (b) HZAC region (c) TMAZ (d) Centre of weld regions [8]

There are less attempt of FSW has been done on dissimilar materials especially between MMCs and aluminum alloy. However, researches were done on dissimilar unreinforced aluminum alloys. Palanivel et al [9] has conducted FSW on AA6351 and AA 5083 H111. The dissimilar joint was produced by FSW machine, keeping AA5083-H111 on retreating side and AA6351 on advancing side as shown in figure 15.

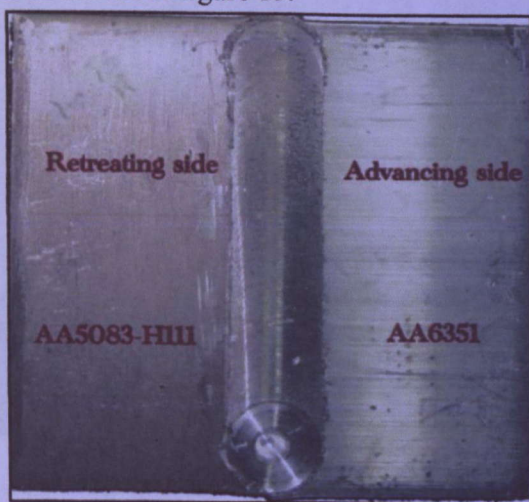


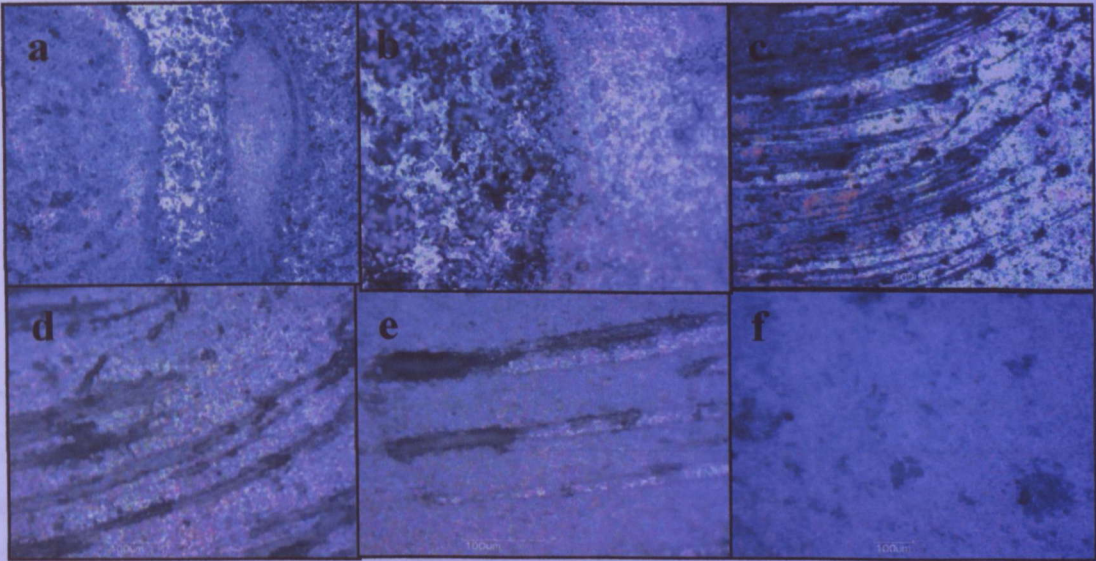
Figure 15: FSW on AA5083H111-AA6351 [9]

The feasible limits of the parameters are given in table 4.

Table 4: Palanivel’s research welding parameters [9]

Tool Rotation Speed	950rpm
Welding Speed	1.05 mm/s
Axial Force	1 tonne

They stated that there were typical features of all different zones in a dissimilar weld cross section of the 6351-Al alloy to 5083-H111A1. The FSP zone shown in the figure 5a was composed of different regions of intense plastic deformation and material flow of both Al-alloys. The grain structure within the FSP was fine and equiaxed the grain size was smaller than in the parent material due to the higher temperature and extensive plastic deformation. Figure 5b depicts the interfacial boundary between the TMAZ and FSP revealing the difference in the grain size clearly. From the figures 5(c)-5(e) the asymmetric pattern of material flow was more clearly observed in the dissimilar weld. The grain structure within the thermo- mechanically affected zone (TMAZ) was elongated and exhibited considerable distortions due to the mechanical action from the welding tool [9].



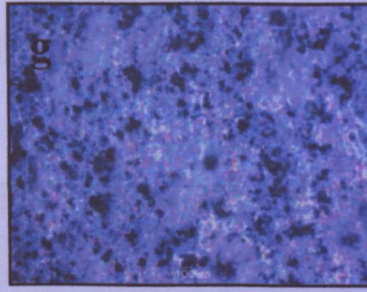


Figure 16: Microstructures view: (a) Composed of different regions (b) TMAZ and FSP (c) Upper portion mixing of two Al alloys (d) Alternative lamellae (e) Upper portion of TMAZ in retreating side (f) Parent material of AA6351 (g) Parent material of AA5083-H111

The research also proved that dissimilar AA6351 and AA5083-H111 aluminum alloy can be welded by FSW without any defect.

Mishra et al. [10] had conducted research on friction stir welding in the aspect of metal flow and microstructure evolution. They proved that the contribution of intense plastic deformation and high temperature exposure within the stirred zone during FSW results in recrystallization and development of texture within the stirred zone and precipitate dissolution and coarsening within the around the stirred zone. Based on microstructural characterization of grains and precipitates, three distinct zones, stirred (nugget) zone, thermo-mechanically affected zone and heat-affected zone (HAZ) as shown in figure 17.

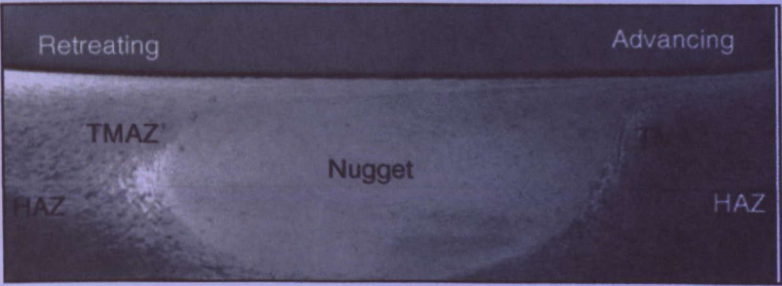
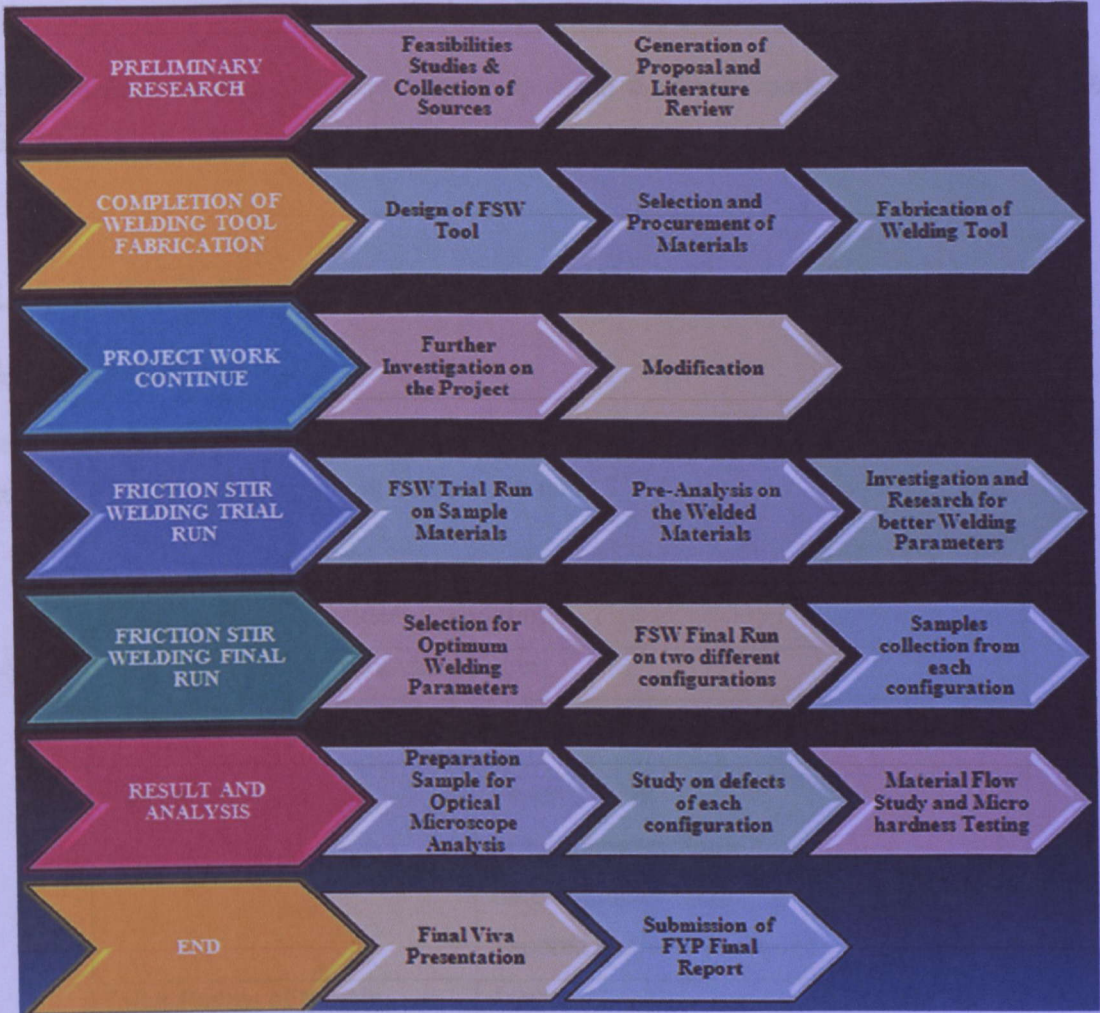


Figure 17: Weld zone [10]

They also stated that in flow visualization in FSW of 2024 Al to 6061 Al, the material flow was described as a chaotic-dynamic intercalation microstructures consisting of vortex-like and swirl features. Apart of that, complex mixing and intercalation of dissimilar metals in FSW were essentially the same as the microstructures characteristics of mechanically alloyed systems.

CHAPTER 3: METHODOLOGY/PROJECT WORK

3.1 Flow Chart/Process Flow



This research focuses on dissimilar material which comprises of aluminum alloy 6092/SIC 25p/T6 metal matrix composite plate and Aluminum Alloy 6061 metal plate.

The researched is initiated with the design of the welding tool using AutoCAD software. Suitable materials were selected and procured before the heat treatment and fabrication of welding tool. AutoCAD design is used to fabricate the welding tool in the laboratory in UTP.

FSW trial run is executed to obtain the acceptable range of welding parameters especially rotation speed and traverse speed. This is to ensure that the final run produced the optimum result for material flow study.

Next, final run of FSW on two different configurations is executed. Cross-section work pieces are taken from both configurations. Microstructures analysis under optical microscope and micro-hardness testing are done to study the material flow of SiC in the weld zone. Findings and results are generated and a detail discussion is be produced.

Lastly, the final result and discussion is compiled in the final report and be presented in final presentation viva to the examiners.

3.2 Friction Stir Welding Tool

3.2.1 Design of Welding Tool

The designed length of the pin is to be 80% of the material thickness and the detail of the selected design of the welding tool is shown in table 5.

Table 5: Design parameters of welding tool

Diameter of the shoulder	20mm
Fillet Radius of the shoulder	2mm
Length of pin	10mm
Design of the pin	Tapered with: Outer diameter 8mm Inner diameter 6mm Tapered angle: 5.71 degree
Fillet Radius of the pin	1mm

Figure 18 illustrates the drawings of FSW tool with dimension using AUTOCAD.

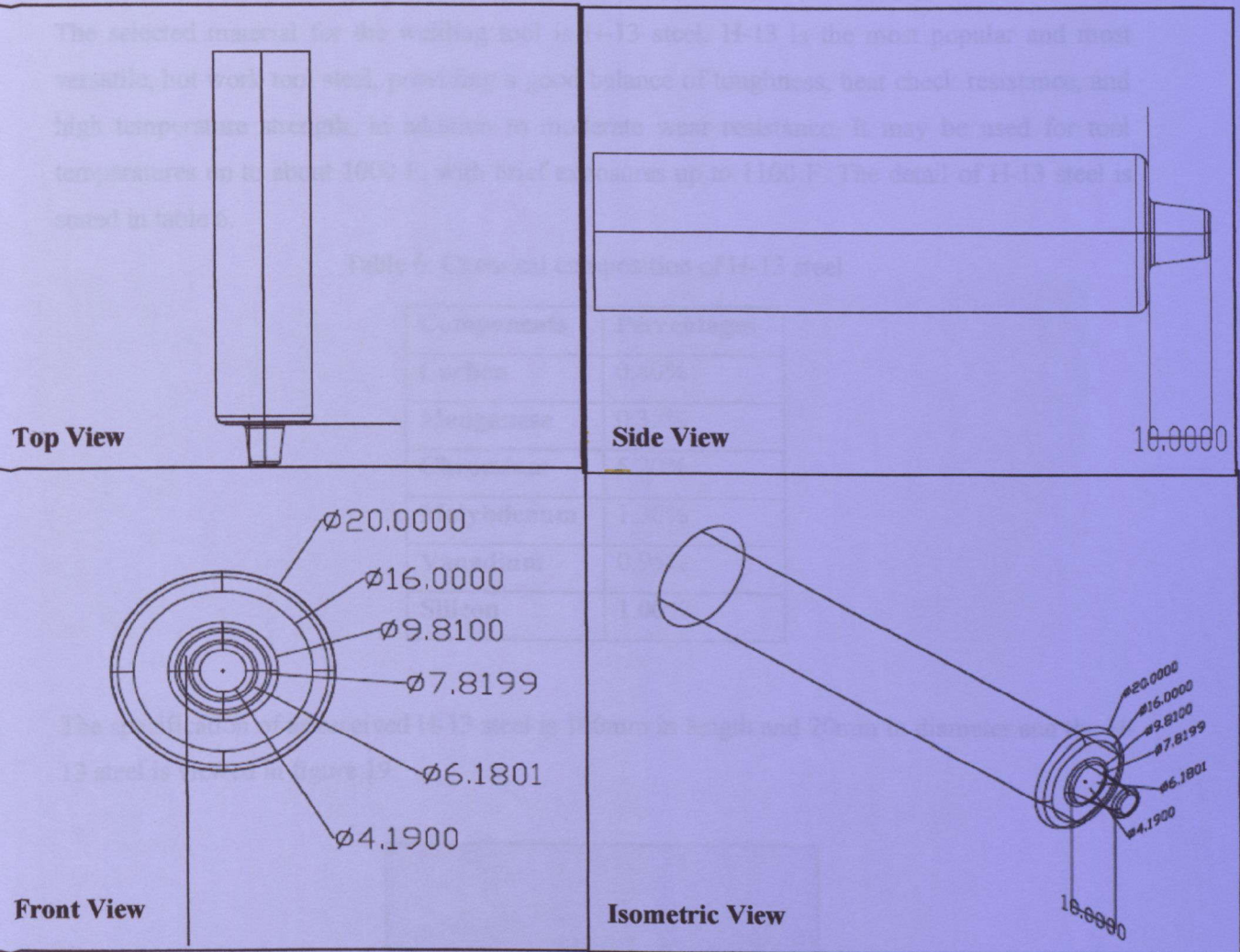


Figure 18: FSW AUTOCAD drawings with dimension in unit of mm

3.2.2 Selection of Welding Tool Material

The selected material for the welding tool is H-13 steel. H-13 is the most popular and most versatile, hot work tool steel, providing a good balance of toughness, heat check resistance, and high temperature strength, in addition to moderate wear resistance. It may be used for tool temperatures up to about 1000 F, with brief exposures up to 1100 F. The detail of H-13 steel is stated in table 6.

Table 6: Chemical composition of H-13 steel

Components	Percentages
Carbon	0.40%
Manganese	0.35%
Chromium	5.20%
Molybdenum	1.30%
Vanadium	0.95%
Silicon	1.00%

The specification of as received H-13 steel is 100mm in length and 20mm in diameter and the H-13 steel is viewed in figure 19.



Figure 19: H-13 Steel

3.2.3 Fabrication & Heat Treatment of Welding Tool

Completion of design and procurement of materials lead to fabrication of welding tool via CNC lathe machine. Figure 20 depicts CNC lathe machine and figure 21 shows CNC coding in panel board that required to be inserted to the machine before it starts to operate. Accurate dimension is required to ensure that the produced tool is the same with the design.



Figure 20: CNC lathe machine

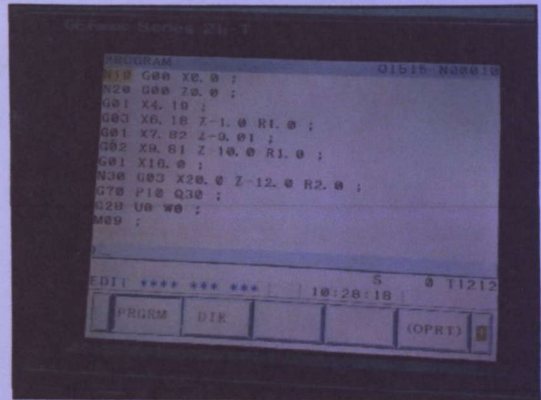


Figure 21: CNC lathe coding and dimensions

Figure 22 is the picture of fabricated welding tool material from CNC lathe machine.



Figure 22: Fabricated welding tool

Heat treatment is required to enhance the hardness of the welding tool. The procedure of heat treatment is as shown:

1. The welding tool is inserted in the Box Furnace and preheated initially for two hours to raise from 0-1350°F [room temperature-732°C]
2. Next, the welding tool is continued preheated; slowly from 1350-1400°F [732-760°C] for another two hours.
3. Then the temperature is raised to 1800°F [1000°C] for one hour
4. Finally it is cooled down to room temperature 75°F (24°C) for two hours

Figure 23 shows box furnace machine with its control unit and figure 24 depicts the welding tool is being placed into the box furnace. Some small piece of ceramics are placed the welding tool to fix the position of the welding tool.



Figure 23: Box furnace with control unit

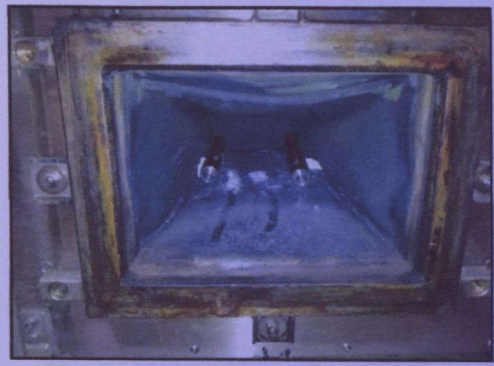


Figure 24: Welding tools in the box furnace

Figure 25 illustrates the welding tool which undergoes heat treatment. Once heat treatment is completed, it is observed that the texture and colour of the surface changed due to oxidation process.



Figure 25: Welding tool after heat treatment

3.3 EDM Wire Cutting of Workpieces

The chosen workpieces are Aluminum Alloy 6061 metal plate and Aluminum Alloy 6092/SIC 25p/T6 metal matrix composite plate. As received plate has dimension of 5inch x 8 inch x 0.5 inches. However, the required dimension for the project is 2.5 inch x 8 inch x 0.5 inches. Hence, the plate was cut in half to obtain the required dimension using wire cut EDM. The results of EDM wire cut are shown in the figure 26 and 27.



Figure 26: AA 6061 after EDM wire cut

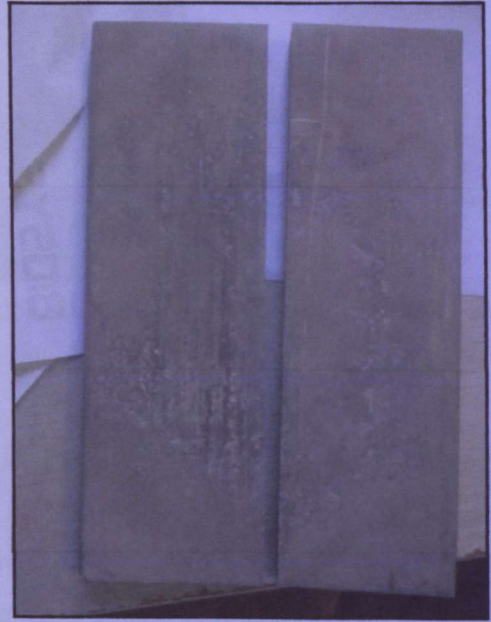


Figure 27: AA 6092 MMC after EDM wire cut

3.4 Friction Stir Welding Clamping System

In FSW, a customized clamping system with specified dimension is needed to fix the position of the materials. Umar et al.[8] had come out with a clamping system to clamp work piece with dimension 0.5 inch x 8 inch x 5 inches. The clamping system is shown in figure 28 and figure 29. This clamping system is to be used for this research as the dimension of the workpiece is within the acceptable range.

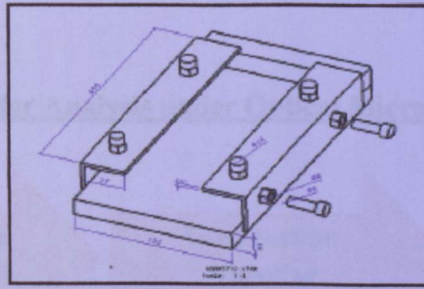


Figure 28: Sketch of customized clamping system with dimensions [8]



Figure 29: Fabricated clamping system

3.5 Friction Stir Welding Joining Process

The main equipment, CNC milling machine, is used to clamp the welding tool firmly and produce rotation on the welding tool. The rotation will produce heat and friction which soften two materials and mix the particles to make the joining. Apart from that, CNC milling machine is able to set some important parameters such as rotation speed, feed rate, dwelling time and penetration depth in panel board as shown in figure 30(a). Figures 30 (b-d) illustrate FSW welding process.

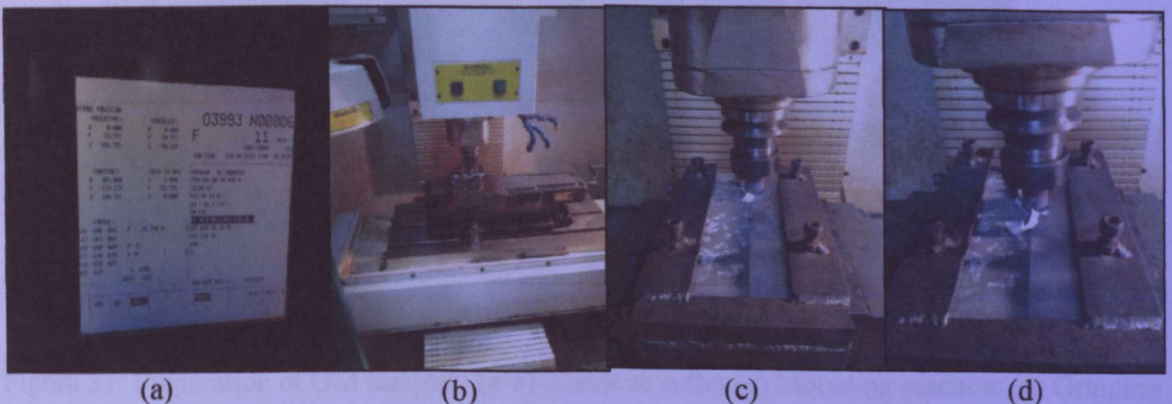
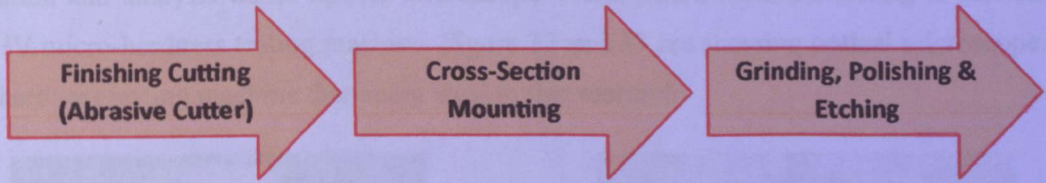


Figure 30: CNC milling machine: (a) Display panel board (b-d) FSW process

3.6 Sample Preparation for Analysis under Optical Microscope



After completion of FSW final run, the welded plates were sent to EDM wire cut before cross-section cutting using abrasive cutter. Abrasive cutter in figures 31(a-b) is used to get the finishing cutting on the cross-section to make sure that the microstructures is not spoiled during the cutting process. Next, the cross-section sample were sent for mounting service where all the cross-sections required are mounted properly before grinding and polishing process. Mounting machine is shown in figure 31(c). The process is followed by grinding and polishing as depicted in figure 31(d) to ensure there is no scratch and impurity on the surface. A proper grinding and polishing process will result sample with mirror effect. The last step is etching process. Kelle Reagent is chosen as the etching reagent. Figure 31 demonstrates the picture of abrasive cutter, mounting machine and grinding process.



Figure 31: Preparation of OM samples: (a-b) Abrasive cutter (c) Mounting machine (d) Grinding process

Once all the processes above are completed, the samples were continued with microstructure observation and analysis under optical microscope. Next, micro-hardness testing is carried out using HV micro-hardness testing machine. Figure 32 and 33 are showing optical microscope and micro-hardness testing machine that being used in this research.

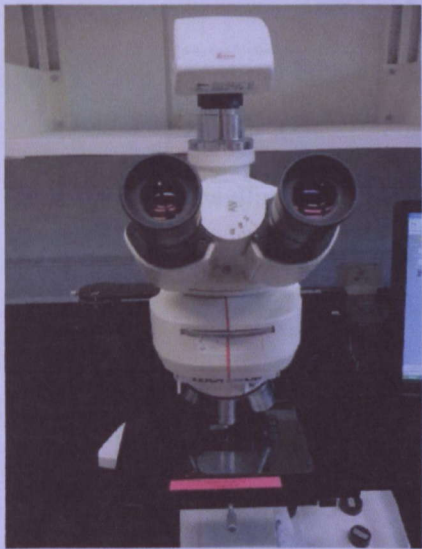


Figure 32: Optical microscope



Figure 33: Micro-hardness testing machine

CHAPTER 4: RESULT & DISCUSSION

4.1 FSW Trial Run & Preliminary Result

Friction stir welding trial run of this project was conducted with the parameters in table 7.

Table 7: FSW trial run parameters

Rotation Speed	1000 rpm
Feed Rate	15 mm per minute
Dwelling Time	10 seconds
Penetration depth	10.1mm

Configuration for FSW trial run is shown in figure 34:

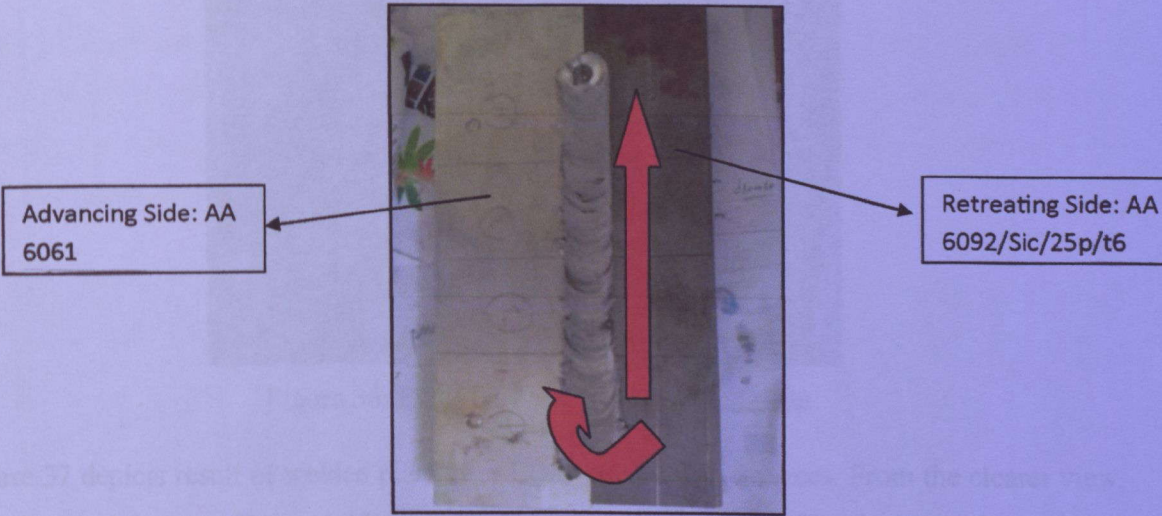


Figure 34: FSW trial run configurations

Dimension of the two materials are varies where dimension of AA 6061 is 0.5inch X 2.5 inches X 8 inches while dimension of AA 6092/SiC/25p is 0.506 inch X 2 inches X 8 inches. Figure 35 illustrates visualize result on the trial run welded surface. The surface had less splash and defect based on the selected parameters. It is expected to be the effect due to the special design of the welding tool which has curvy surface at the shoulder touching surface. The welded plate is the cut into four pieces using EDM in order to observe the defect and structures of the weld zone.



Figure 35: Result of FSW trial run surface

As shown in figure 36, sparks occurred during the EDM wire cut and water was required to cool down the temperature of the welded plate in the process.



Figure 36: EDM wire cut on the welded plate

Figure 37 depicts result of welded plate after EDM cutting into 4 pieces. From the clearer view, it is observed that non-linear welding surface as shown in figure 35. This is due to the variation of the material thickness and cause less shoulder contact at the advancing side (AA 6061) and brought to phenomena in figure 36. Apart from that, the trial run result is affected by improper clamping of the materials. The used material has 2 inch width which is 0.5 inch less than the required length of the material. The reduction of width is due to improper cutting tool is selected in cutting the AA 6092/Sic/25% metal plate.

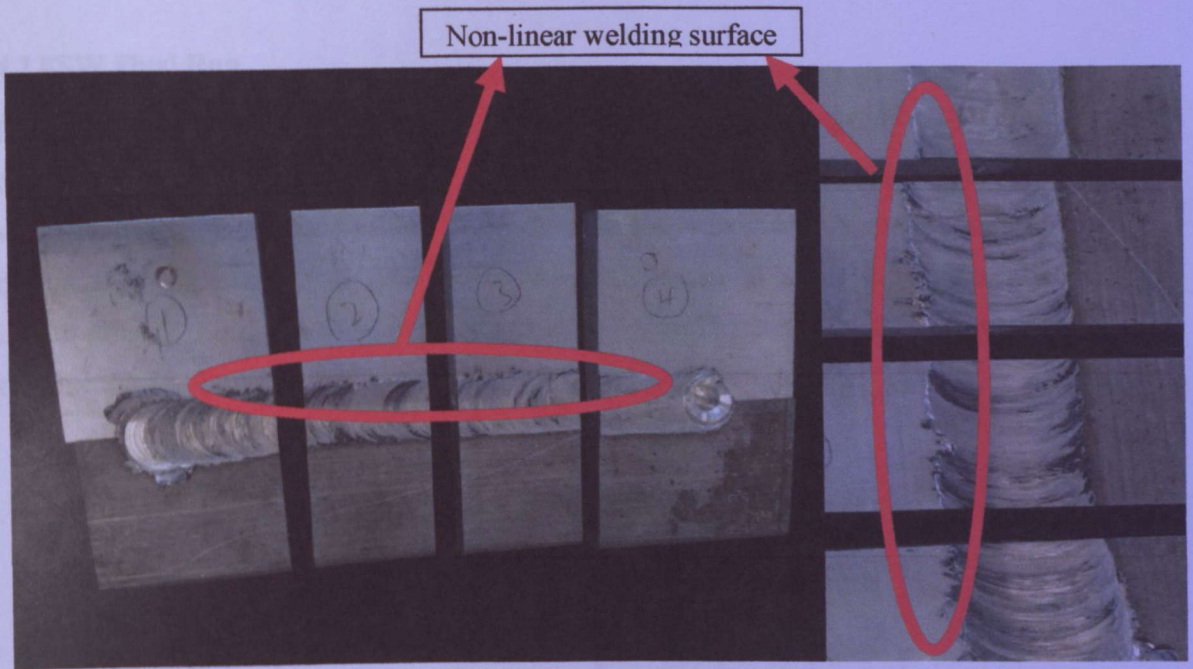


Figure 37: Welded plate of trial run after EDM cutting into 4 pieces

Figure 38 demonstrates that there is tunnel defect that appeared at the advancing side of the welded plate. The circled area shows that the tunnel hole had almost the same shape and size in the whole weld zone area from part 1 to part 4 (parts labeled in figure 35). The occurrence of the weld hole might due to the high feed rate speed.

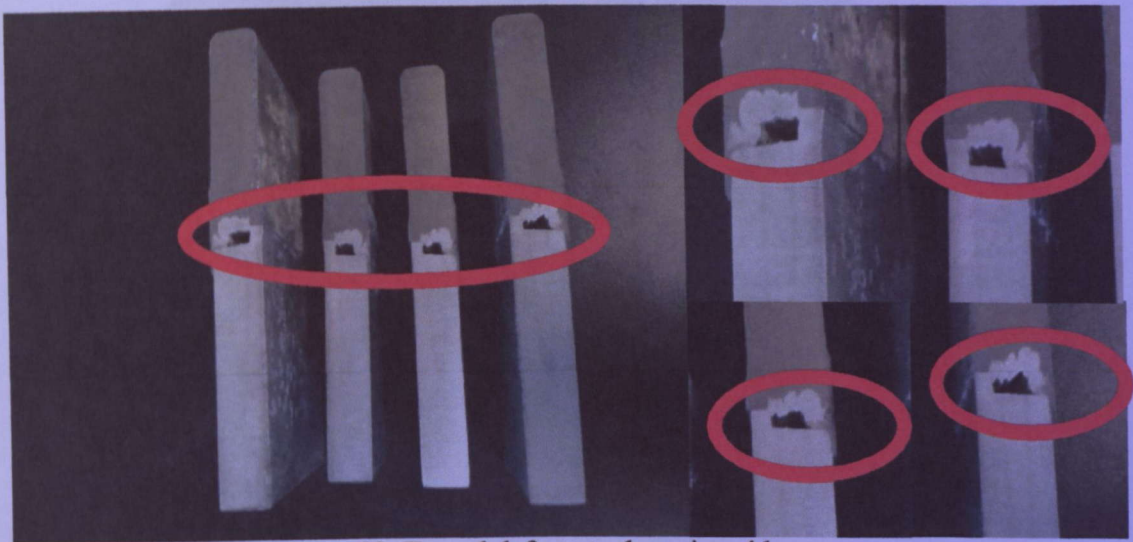


Figure 38: Tunnel defect at advancing side

4.2 FSW Final Run

Based on pre-analysis and research done on the result of trial run result, some adjustment was done on the FSW final run parameters as shown in table 8. Rotation speed was increased by 20% while feed rate is decreased by 20%. This is to ensure that there is enough heat and stirring effect during FSW process. Apart from that, dwelling time is doubled and penetration depth is increased by 0.1mm. The changes were predicted to give enough heating and softening process to solve the dissimilar materials depth problem.

Table 8: FSW final run parameters

Rotation Speed	1200 rpm
Feed Rate	11.25 mm per minute
Dwelling Time	20 seconds
Penetration depth	8.2mm

Two types of configurations are conducted for this project. The FSW final run result is shown in the figure 39.

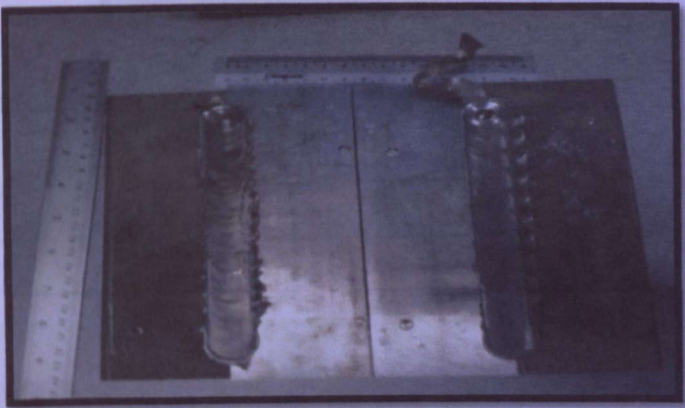


Figure 39: FSW final run welded plates

4.3 Configuration 1

Figure 40 depicts configuration 1 in FSW final run. In configuration 1, AA6061 was located as advancing side while AA6092 MMC was located as retreating side using the final run parameters.

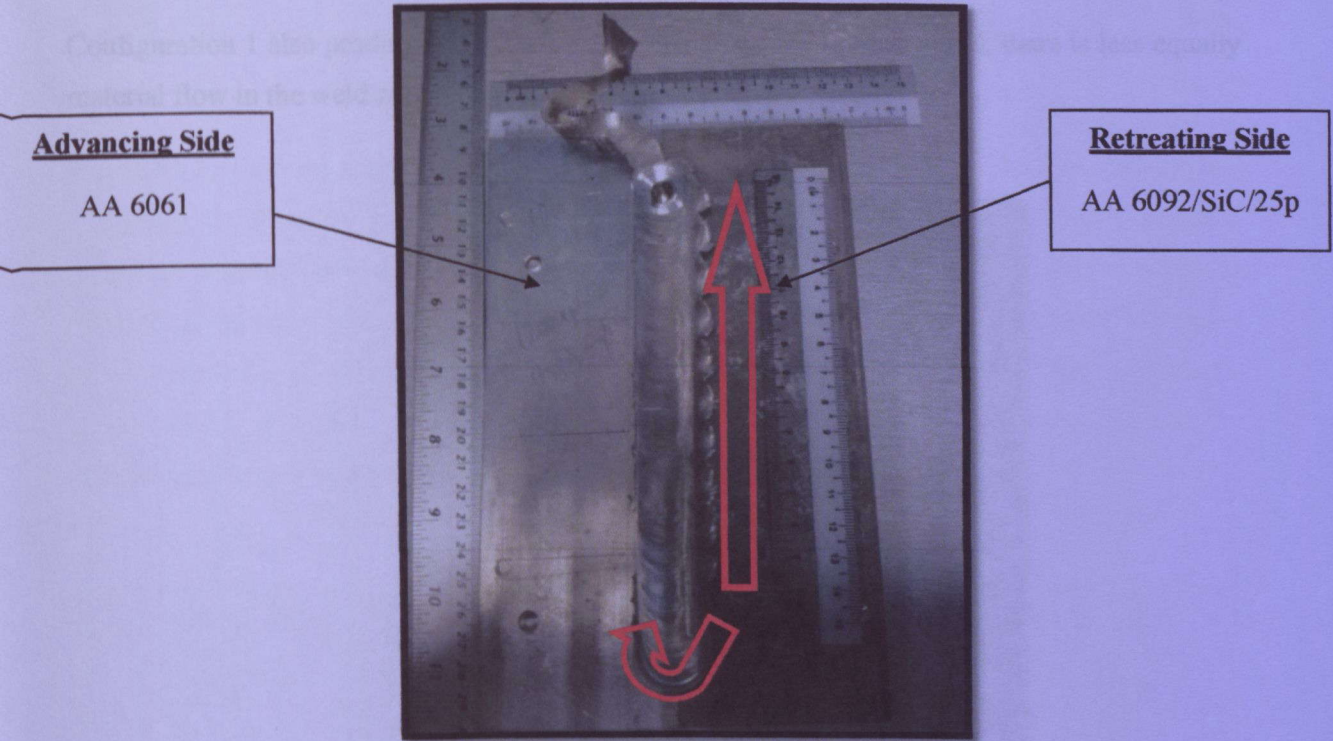


Figure 40: Illustration of FSW configuration 1

Figure 41(a) illustrates that configuration 1 has splash occurred at retreating side and no splash is occurred at advancing side. Furthermore, configuration 1 produced smooth and clean weld surface at weld zone as shown in figure 41(b).

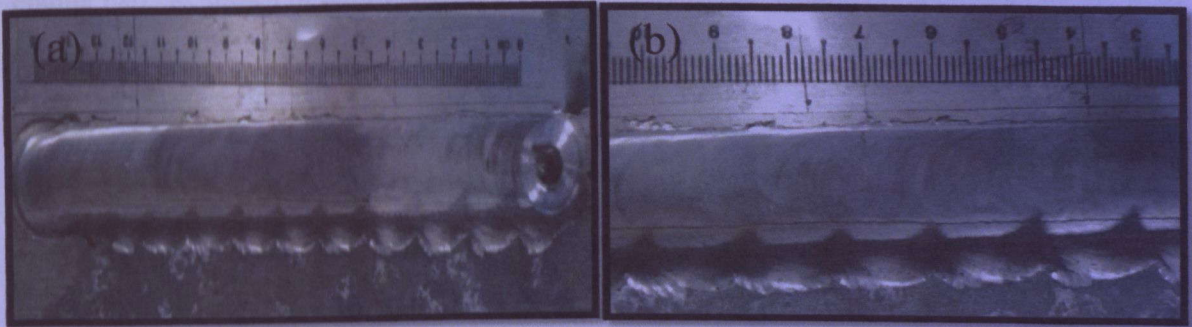


Figure 41: FSW weld surface in configuration 1: (a) Splash at retreating side (b) Smooth weld surface

However, configuration 1 depicts a long splash at the advancing side in the end of the FSW as shown in figure 40. The splash is accumulated from the starting to the end and it illustrates an estimated 8cm long splash. It is believed that this long pattern splash at the end point brought zero splashes along the weld surface.

Configuration 1 also produces defect hole in the weld zone. In other words, there is less equal material flow in the weld zone. The defect hole is shown in figure 42.



Figure 42: Defect hole in FSW configuration 1

After completion of FSW, the weld zone is cut to cross sections at the beginning, middle and ending parts as shown in the figure 43. It is clearly shown that a tunnel is spotted along the weld zone and black silicon carbide particles are spotted in the tunnel. The spotted silicon carbide particles show inefficient mixture of SiC particles in the weld zone. The defect hole is mostly due to insufficient heating and low temperature. Apart from that, the shape of weld hole is constant from beginning until the ending but the size varies. Figure 43 illustrates that the middle point of the weld zone has smallest weld hole and this proves better welding result at the middle point of weld zone.



Figure 43: Cross-section of configuration 1 from starting to ending

Figure 44 depicts the result of the cross-section mounting after grinding, polishing and etching. Mounting A, B and C in figure 44 shows that there are different patterns of SiC particles distribution at different area of SiC. Mounting A has a clear SiC particles distribution line between nugget zone and TMAZ area in advancing side. The line which is shown in mounting A shows concentration of SiC particles and it is proven by observation under optical microscope (OM). Apart from that, there are more SiC particles distribution from retreating side to advancing side in Mounting B as compared to mounting A and C.

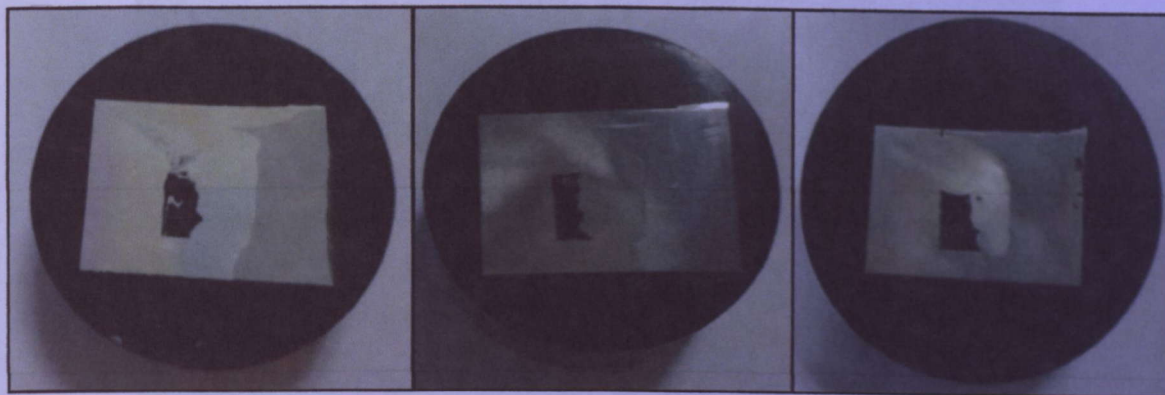
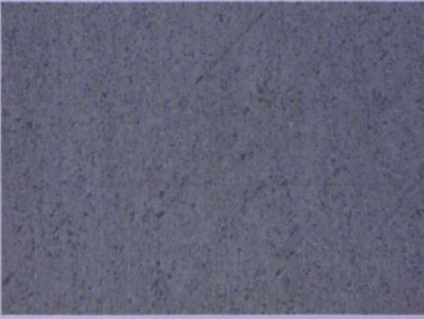


Figure 44: Cross-section in mountings A,B,C : (A) Beginning point (B) Middle point (C) Ending point

Figures 45 (a) and (b) illustrate OM pictures of parent materials of AA6061 and AA6092 MMC. It is shown that there are no SiC particles in AA6061 while SiC particles are distributed randomly in AA6092 MMC.

(a)



(b)



Figure 45: Parent material under OM 50X: (a) AA6061 (b) AA6092 MMC parent material under OM

Figure 46 demonstrates SiC distribution line between nugget zone and TMAZ area at advancing side. This has proven that SiC particles are circulated to advancing side during FSW joining process and it is only concentrated at that particular distribution line.

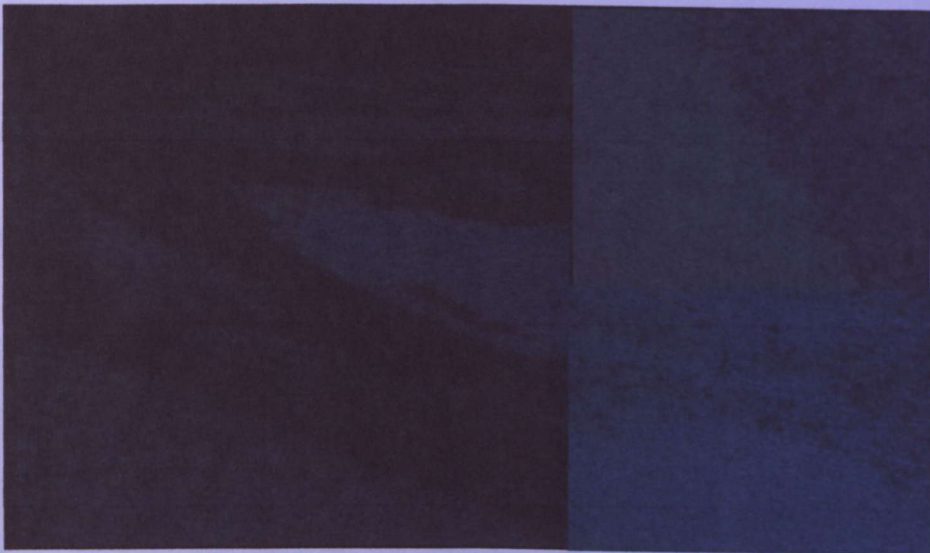


Figure 46: SiC distribution line between nugget zone and TMAZ area at advancing side for 5X, 10X and 50X under OM

Figure 47(a) shows concentration of SiC particles in nugget zone before the transition line. It is clearly seen that the particular area is covered by both large and small size of SiC particles as compared to the AA6092 MMC parent material. It is predicted that the stirring of FSW has gathered SiC particles at nugget zone and this will explain the presence of compact SiC particles at weld zone. Apart from that, figure 47(b) illustrates clear transition zone in the nugget area. It is clearly shown a separation line between the nugget zone. Beyond the transition line in advancing

side shows no presence of SiC particles and this proved that distribution of SiC particles is limited at advancing side.

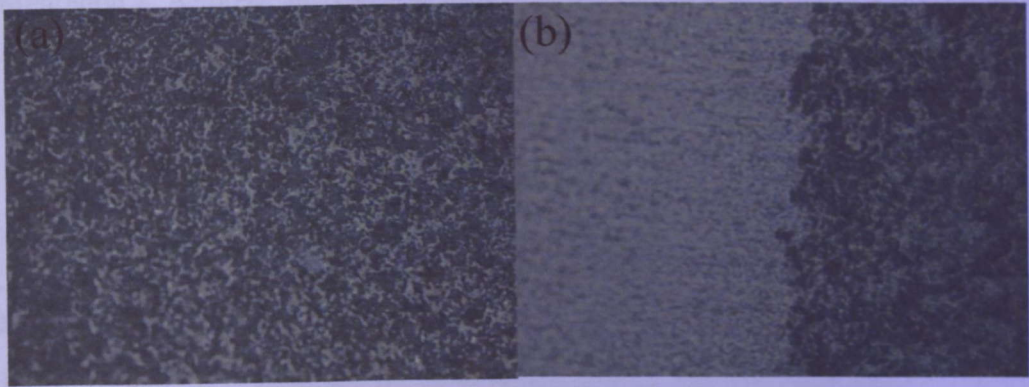


Figure 47: SiC distribution: (a) Concentration of SiC at nugget zone (b) Transition zone in nugget area

Figure 48(a) illustrates unaffected zone in advancing side has no presence of SiC particles. It shows that there is almost no SiC particles are found in advancing side beyond the transition line shown in figure 47(b). Figure 48(b) depicts that HAZ area at retreating side has almost the same picture under OM with parent material 6092 MMC. Amount of SiC particles are almost the same with large and small size of SiC particles. This can prove that there is limited circulation of SiC particles from HAZ and TMAZ area from retreating side to advancing side.

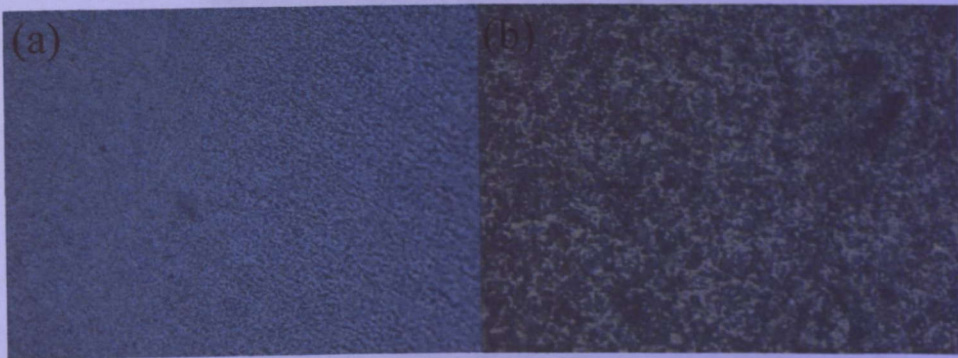


Figure 48: SiC distribution: (a) Unaffected zone in advancing side (b) HAZ & TMAZ area at retreating side

4.4 Configuration 2

In configuration 2, AA6092/SiC/25p was located at advancing side while AA 6061 was located as retreating side during the FSW using same parameters stated as in configuration 1. The illustration of configuration 2 is shown in the figure 49.

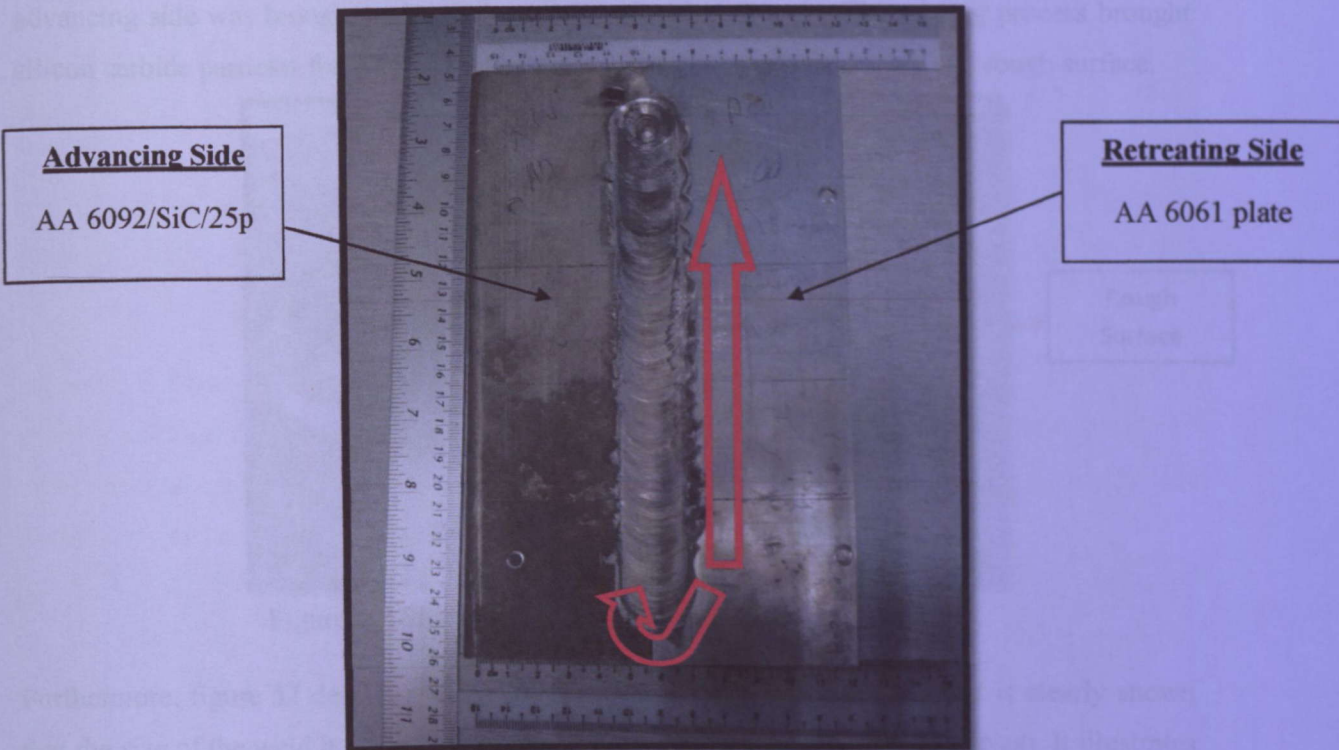


Figure 49: Illustration of FSW final run configuration 2

Figure 50 depicts that there is splash occurred at retreating side while there is only little splash occurred at advancing side.

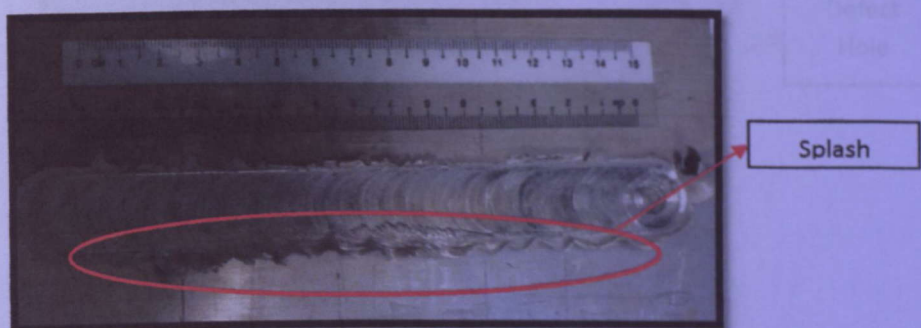


Figure 50: Splash at retreating side at configuration 2

Figure 51 illustrates distribution of silicon carbide particulates was seen by eye visual inspection. The black colour particles shows silicon carbide particles in the nugget weld zone. Apart from that, it is shown that the weld zone surface was rough. This result is supported by the research by Prater [6]. In his paper, he claimed that FSW on MMC will produce rougher surface. In this configuration, AA6092/SiC/25p MMC as advancing side, therefore, silicon carbide from advancing side was brought and distributed over the nugget zone. The stirring process brought silicon carbide particles from MMC to the surface and hence produce black and rough surface.

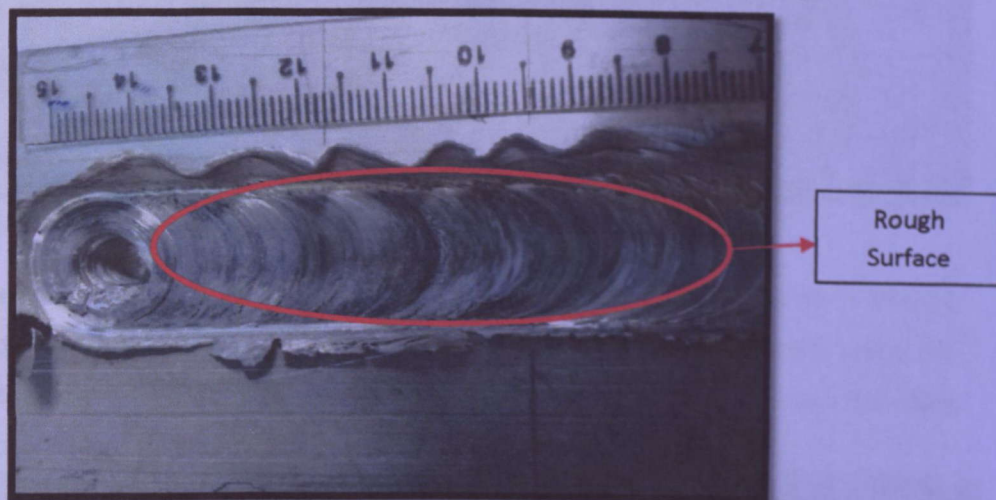


Figure 51: Silicon carbide particles at weld zone surface

Furthermore, figure 52 depicts a tiny weld hole that valid in the weld zone. It is clearly shown that the size of the weld hole is greatly decreased as compared to the trial run result. It illustrates that the decrease in feed rate brings effect in reducing the weld hole.

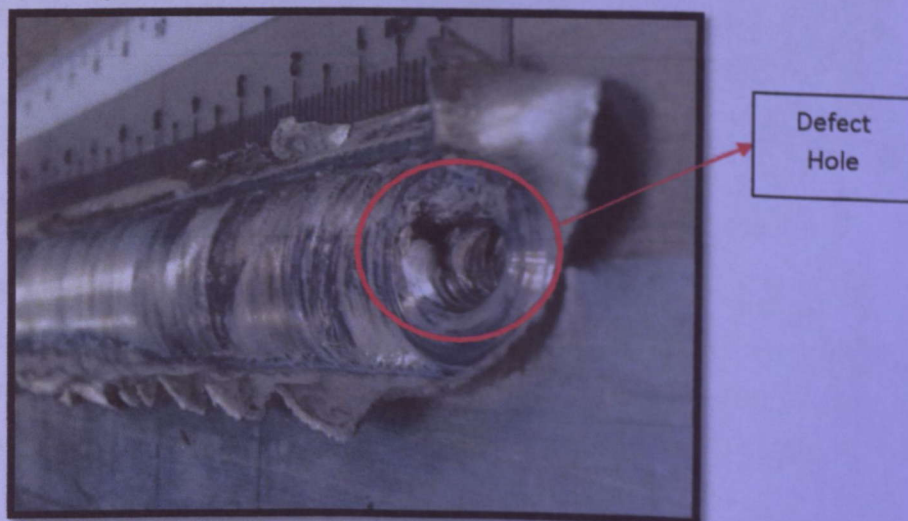


Figure 52: Defect hole in FSW configuration 2

Figure 53 shows that there is a very small defect spotted at the ending point of weld zone and there are no defects and weld hole are spotted at the middle and beginning of weld zone. Even though weld zone is spotted as shown in figure 53, there is no tunnel effects spotted in the cross-section.

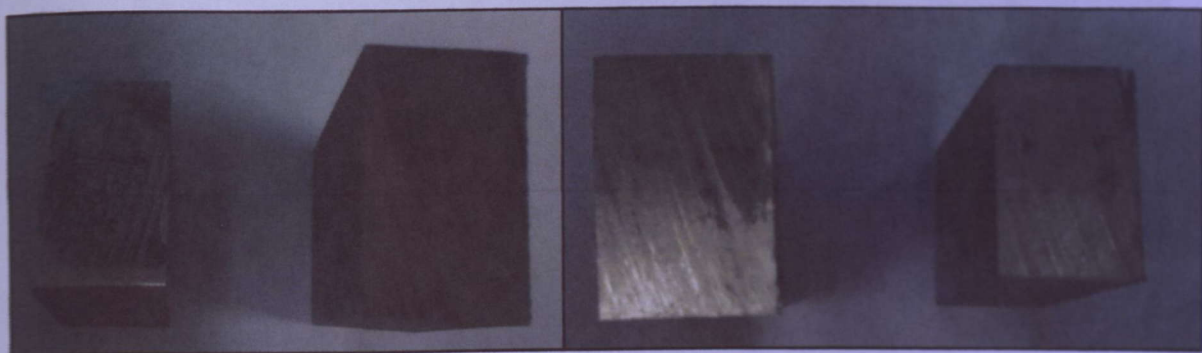


Figure 53: Cross-section of configuration 2 from starting to ending

Figures 54 illustrates the pattern of SiC particles distribution is different in mounting D,E and F but the distribution area is almost the same along the weld zone. Mounting E has more SiC circulation as compared to mounting D and mounting E. From visual observation, configuration 2 has more area covered by SiC particles as compared to configuration 1.

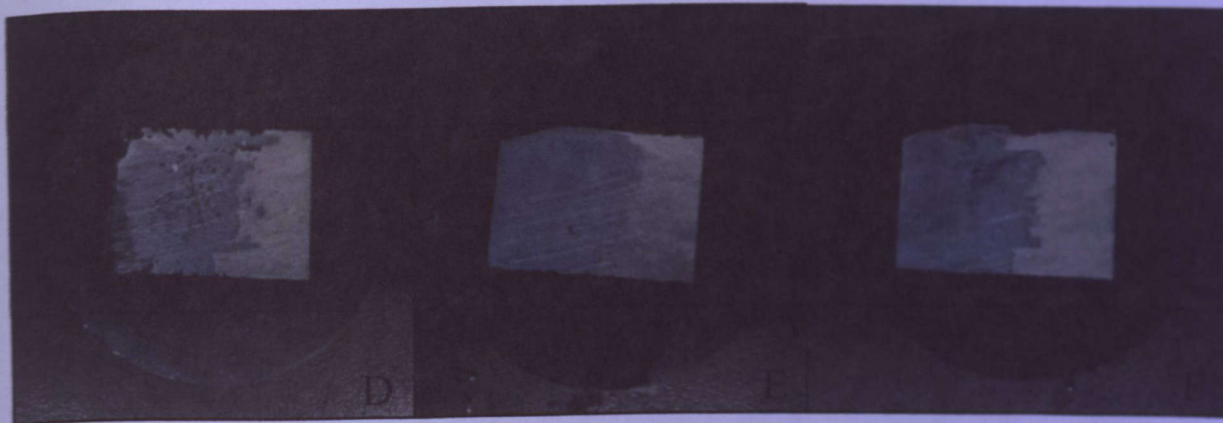


Figure 54: Cross-section mountings D, E, F: (D) Beginning point (E) Middle point (F) Ending point

FSW stirring effect has made a clear SiC distribution line as shown in figure 55(a) while figure 55(b) presents the transition zone at weld nugget in configuration 2. Figure 55(a) proves that that some small SiC particles are circulated beyond the transition line in weld nugget. In other words, mixtures of SiC particles are spotted at retreating side after the transition line in weld nugget.

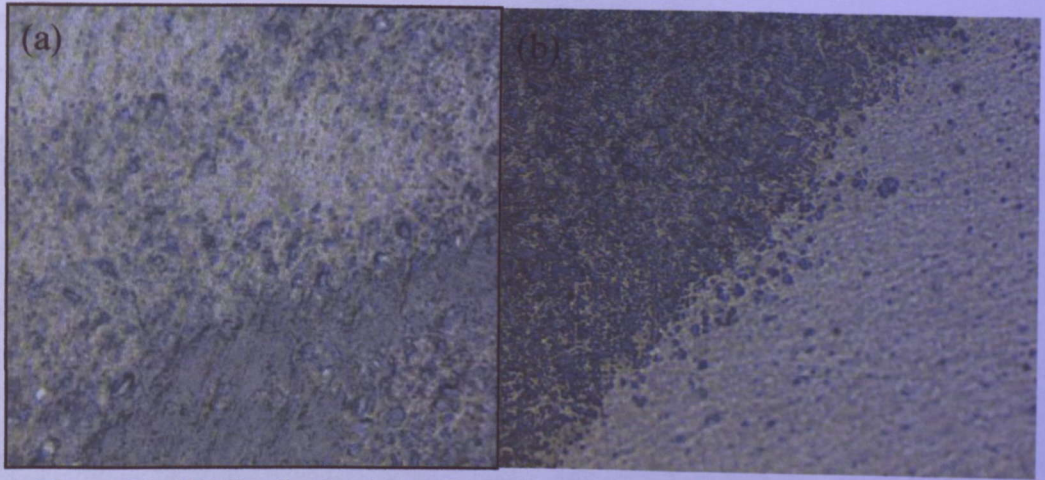


Figure 55: SiC distribution in configuration 2: (a) Clear SiC distribution line (b) Transition Zone at Weld Nugget

Figure 56(a) depicts that there is high concentration of SiC particles gathered at nugget zone. The spotted SiC particles are more compact as compared with AA6092 MMC parent material in figure 45(b). There are little small size SiC particles found in advancing side. It is predicted that small SiC particles tends to be circulated from advancing side to the nugget zone. This phenomenon is proven by figure 56(b). It proves that large SiC particles are left at advancing side. As compared with AA6092 MMC, figure 56(b) illustrates more large particles but little small size of SiC particles.

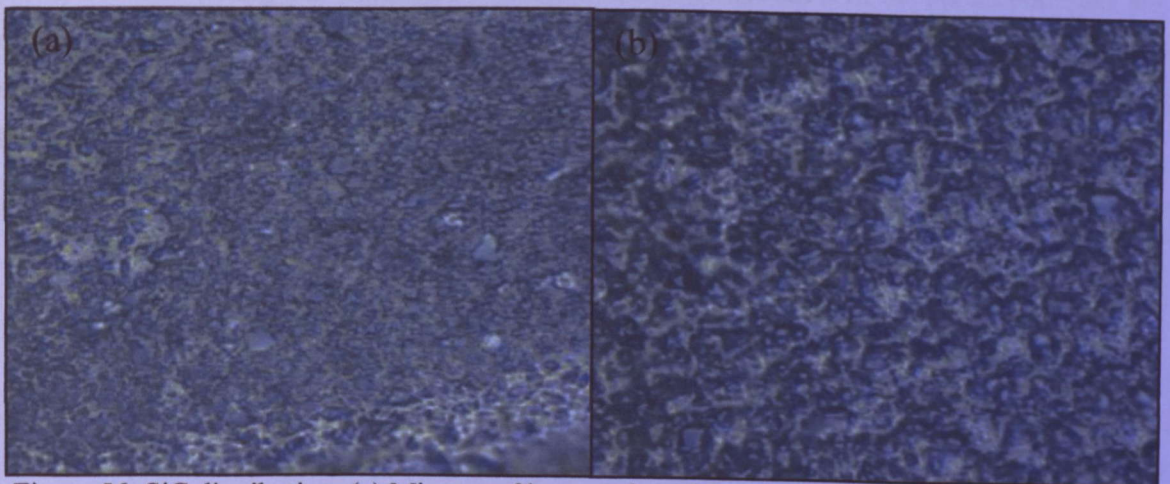


Figure 56: SiC distribution: (a) Mixture of large and small SiC particles (b) Large SiC particles at Advancing Side

Figure 57 demonstrates that some small SiC particles are spotted at TMAZ, HAZ and unaffected zone in retreating side. It is clearly shown that the SiC particles from advancing side are being circulated to retreating side. As compared with AA6061 parent material in figure, it clearly

shows that the mixture of SiC particles. Amount of SiC being circulated is uncountable but it is less as compared to weld nugget zone in figure 57(a).

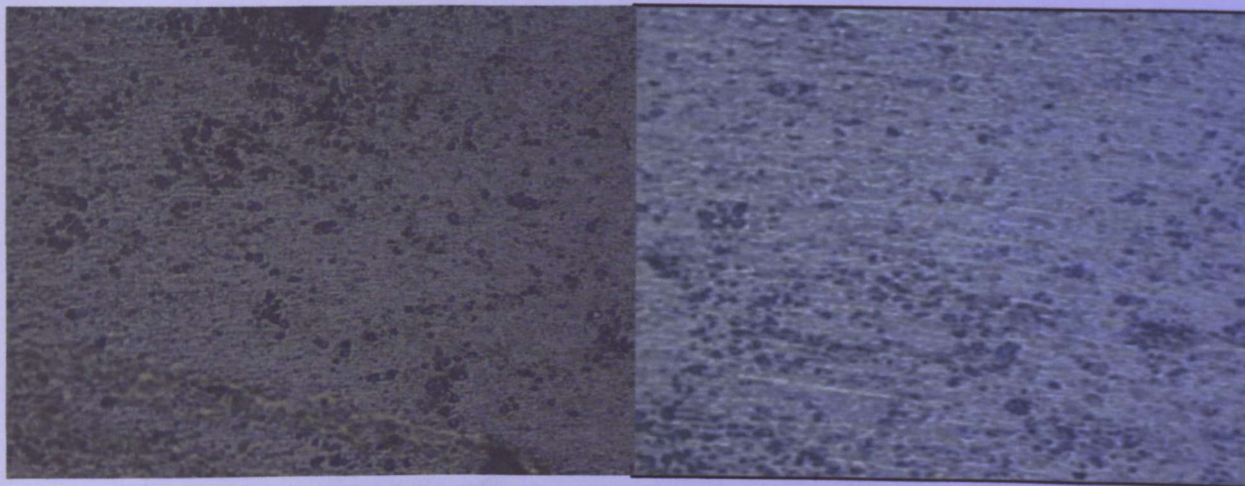


Figure 57: Small SiC particles spotted at retreating side

4.5 Micro-hardness Testing Along the Weld Zone For Both Configurations

Micro-hardness testing was conducted to evaluate the micro-hardness of the parent materials and different location at weld zone in each configuration. SiC is reinforcement particles which can enhance the hardness of the material. It is predicted that the location with more SiC particles will have higher HV value. Micro-hardness testing of parent materials has been done as reference. The HV value for each parent material is listed as below:

Table 9: HV value of AA6061 and AA6092 MMC parent material

AA 6061 Plate	58.3 HV
AA 6092/SiC/25p MMC	135HV

Figure 58 demonstrates the result for micro-hardness testing along the weld zone for both configurations.

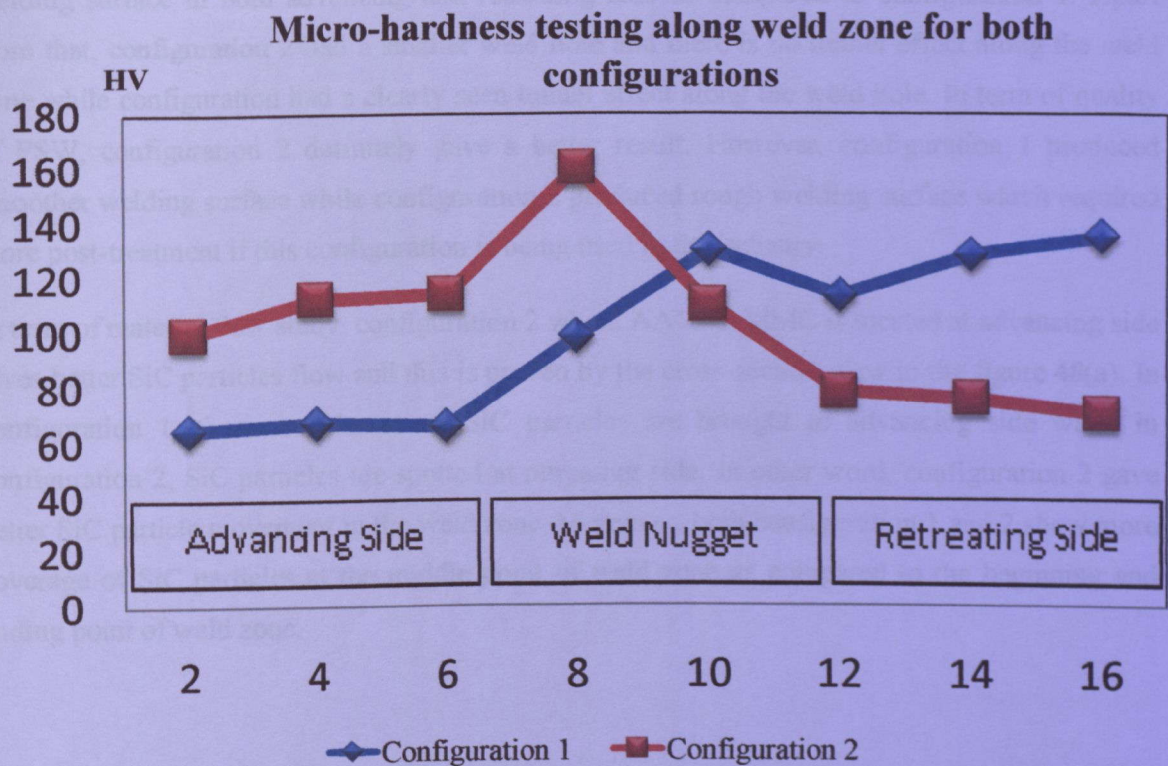


Figure 58: Micro-hardness testing along weld zone for both configurations

It is showed that HV value in configuration 1 is increasing from advancing side to retreating side as SiC particles is increasing along the path. Meanwhile, the graph is decreasing from advancing to retreating side in configuration 2 as SiC particles is reducing along the path. In both configurations, there is a sudden rise in weld nugget as the concentration of SiC particles are spotted at the weld nugget. The HV value in the high peak is higher than HV value of AA6092 MMC as more SiC particles are present in the spot as compared with the parent material. Apart from that, HV value in retreating side in configuration 2 is higher than AA 6061 parent material as some little amount of SiC particles are spotted at that area and it give a slight rise in HV value. While advancing side in configuration 1 has almost the same HV value with AA6061 parent material and it depicts no SiC particles presence here. The greater SiC particles circulation in configuration 2 also was shown by the higher HV value at AA6061 side in configuration 2.

4.6 Comparison and Discussion between Both Configurations

From visual observation on the welding result, configuration 2 produced less splashes on the welding surface in both advancing and retreating side as compared to configuration 1. Apart from that, configuration 2 had a smaller weld hole and there is no tunnel effect along the weld zone while configuration 1 had a clearly seen tunnel effect along the weld hole. In term of quality of FSW, configuration 2 definitely gave a better result. However, configuration 1 produced smoother welding surface while configuration 2 produced rough welding surface which required more post-treatment if this configuration is being used in the industry.

In term of material flow study, configuration 2 which AA6092 MMC is located at advancing side gives better SiC particles flow and this is proven by the cross-section view in the figure 48(a). In configuration 1, there are almost no SiC particles are brought to advancing side while in configuration 2, SiC particles are spotted at retreating side. In other word, configuration 2 gave better SiC particle movement in the weld zone. Moreover, both configuration 1 and 2 show more coverage of SiC particles at the middle point of weld zone as compared to the beginning and ending point of weld zone.

4.7 Analysis and Discussion on FSW Tool

Figures 59 and 60 demonstrate the transformation and changes of FSW welding tool before trial run, after trial run and after final run. After trial run, the diameter of the pin remains as 6mm at the bottom of the tapered part and 8mm at the top of the tapered part. In figure 48, it is clearly shown Aluminum particles are stuck to the welding tool. Even though the diameter of the pin remains, there is possibility that the pin defects and the defects of the pin is covered by aluminum particle. Furthermore, the height of the pin is remained as 10cm. In other word, there is no defect on the length of the pin. In figure 60, it is clearly seen that diameter of the pin is decreased after final run of FSW. Figure 60 illustrates non-uniform curve at the pin area. Apart from that, diameter of shoulder is reduced after FSW final run. Surface area of the shoulder is worn away during the stirring process. This result is fully supported by Tracey et al. [7]. In their research, it proved that H-13 welding tool is not suitable to be used for too long welding path.

From this research, it also proven that H-13 welding tool could not be used for continuous friction welding. For a long term FSW in industry work, a better tool material should be used such as tool with diamond coating.

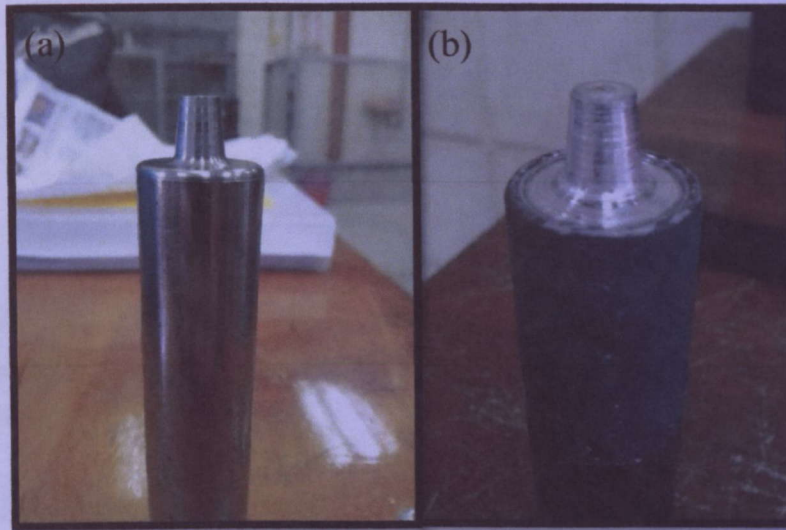


Figure 59: FSW tool (a) before trial run (b) trial run

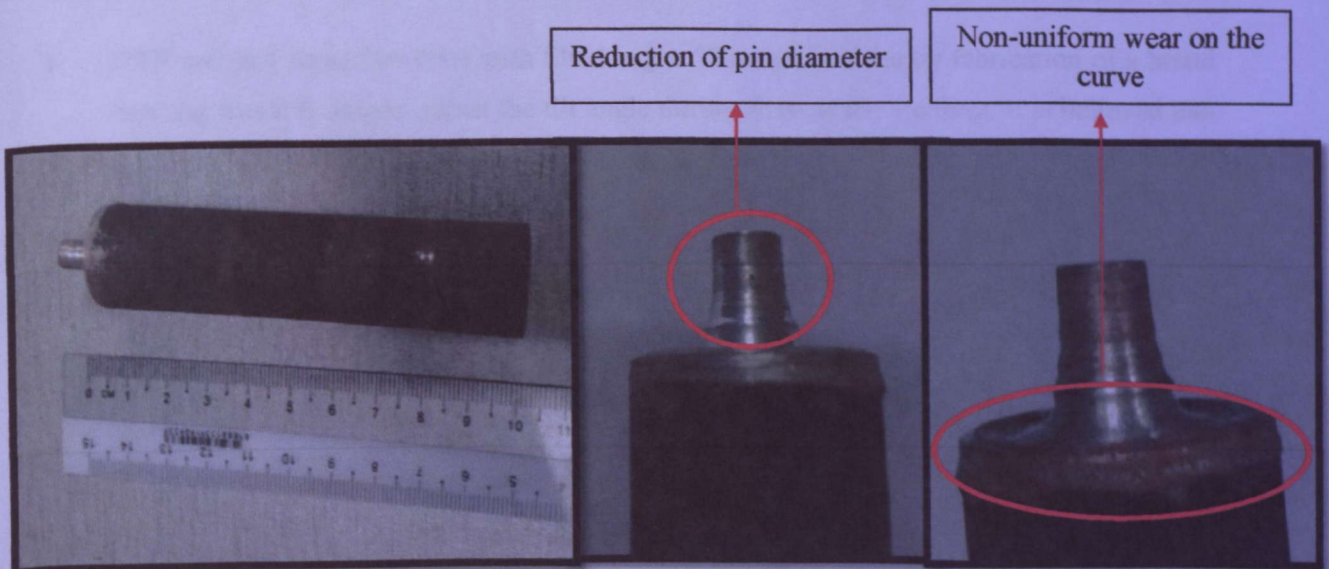


Figure 60: FSW tool after FSW final run

CHAPTER 5: CONCLUSION & RECOMMENDATIONS

5.1 Conclusion

In conclusion, the research has been successfully carried out in six months and the main objective which is to study the SiC particles distribution at the weld zone for two different configurations was achieved. Configuration 2 resulted better FSW result with less wear at surface and minimal weld hole spotted. However, smoother welding surface spotted in configuration 1. SiC particles flow in FSW weld zone in both configurations is not constant in term of pattern and quantity. Apart from that, there is more SiC particles circulation from advancing side to retreating side in configuration 2 where AA6092 MMC is located at advancing side. Furthermore, micro-hardness testing in the research demonstrates that configuration 2 produced average higher HV value as compared to configuration 1 and the zone with more SiC particles will give higher HV value.

5.2 Recommendations

Several recommendations could be raised to improve the result of FSW in the next research. The recommendations are stated as below:

- FSW welding should be done with tilted angle. This can be done by fabrication of a brand new jig which is able to adjust the tilt angle during friction stir welding. It is believed that tilt angle would be able to eliminate weld hole and tunnel effect in the weld zone
- Welding Tool should be fabricated with better materials so that no wear and diameter reduction on pin and shoulder after Friction Stir Welding. Wear and diameter reduction of the tool might affect the result of FSW.

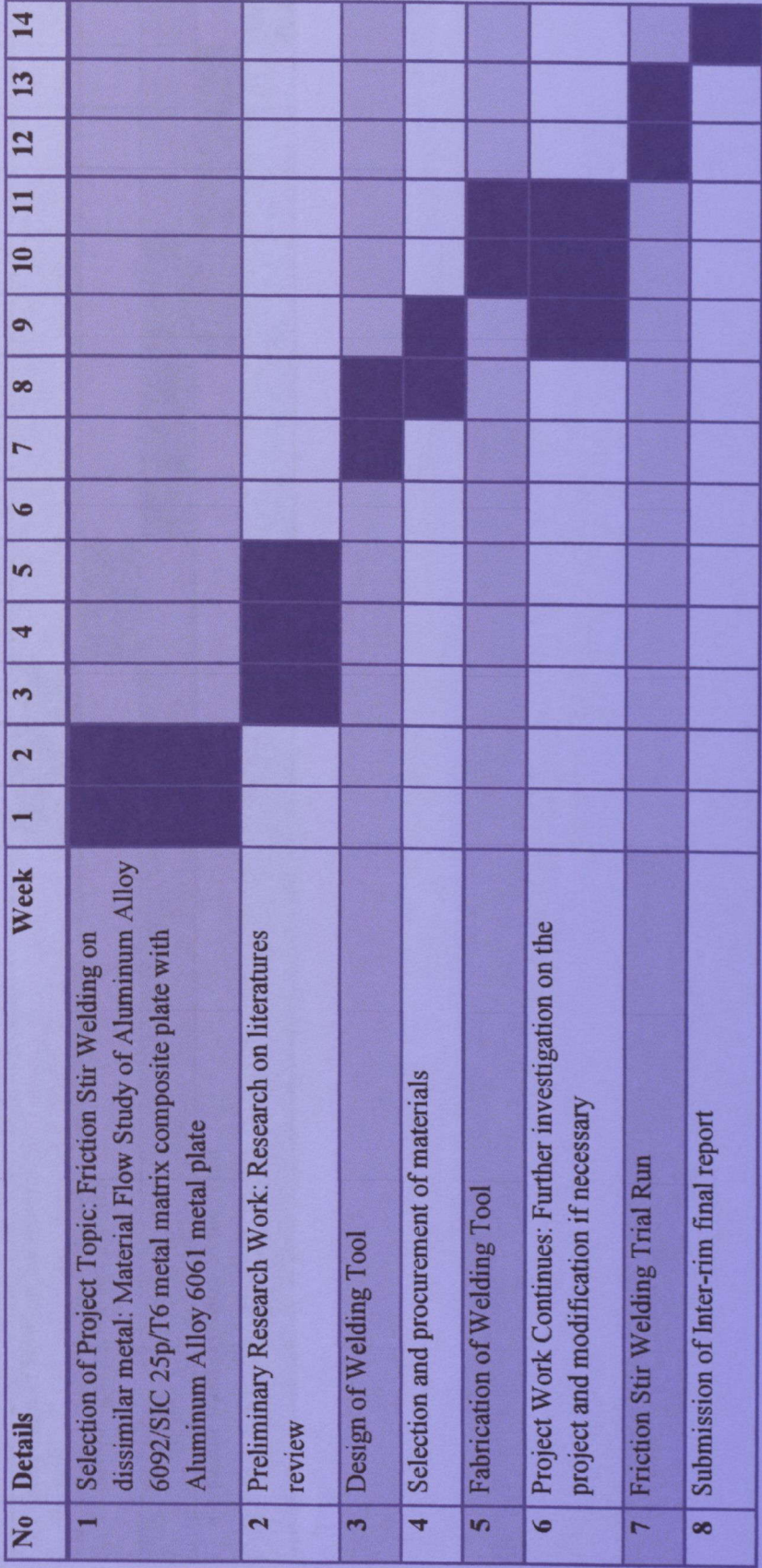
REFERENCES

1. Palanivel, R., Mathews, P.K. & Murugan, N. (2010). Development of mathematical model to predict the mechanical properties of friction stir welded AA6351 aluminum alloy. *Engineering Science and Technology Review*.
2. Emam, S.A. & Domiaty, A.E.(2009). A refined energy-based model for friction stir welding. *World Academy of Science, Engineering and Technology*.
3. Babu, N.B, Kumar, A.P. & Davidson, M.J. (2011). A review of friction stir welding of AA6061 Aluminum Alloy. *Asian research publishing network*.
4. Munoz, A.C. , Ruckert, G , Huneau, B. ,Sauvage, X. & Marya, S.(2008) . Comparison of TIG welded and friction stir welded Al-4.5Mg-0.26Sc alloy. *Journal of materials processing technology* 197.
5. Marzoli, L.M., Strombeck, A.V., Santos, J.F., Gambaro, C. & Volpone, L.M. (2006). Friction stir welding of an AA6061/Al₂O₃/20p reinforced alloy. *Composites Science and Technology* 66.
6. Prater, T.(2008). An investigation into the friction stir welding of Al 6061 and Al 6061/SiC/17.5p using diamond coatings. *Graduate School of Vanderbilt University*.
7. Tracy, W.N & Dick, L.(2009). Friction Stir Welding of Aluminum MMC 6092-17.5% SiC_p. *Brigham Young University Provo UT*.
8. Umar, B.P & Mokhtar, A. (2011). Friction Stir Welding on Aluminum 6092/SiC/25p/t6 Metal Matrix Composite: its microstructure evolution and mechanical properties. *Mechanical Engineering Universiti Teknologi Petronas*.
9. Palanivel, R., Mathews, P.K. & Murugan, N. (2010). Influences of tool pin profile on the mechanical and metallurgical properties of friction stir welding of dissimilar aluminum alloy. *International journal of engineering science and technology*.
10. Mishra, R.S & Ma, Z.Y. (2005). Friction stir welding and processing. *Master Science and Engineering RSO*.

APPENDIXES

Gantt Chart

FYP 1



FYP 2

No	Details	Week	1	2	3	4	5	6	7	8	9	10	11	12	13	14
1	Final run of FSW on the material															
2	Sampling from welded material															
3	Microstructures Analysis															
4	Result and discussion on the result															
5	Submission of FYP final report															

Project Milestones

FYP 1

No	Details Week	1-5	6	7	8	9	10	11	12	13	14
1	Completion of Procurement of Materials						23 Mar 2012				
2	Completion of Fabrication of Welding tool								6 April 2012		
3	Completion of Friction Stir Welding Trial Run										27 April 2012

FYP 2

No	Details Week	1-5	6	7	8	9	10	11	12	13	14
1	Completion of FSW final run		25 June 2012								
2	Completion Microstructure Analysis and Microhardness testing						27 July 2012				
3	Completion of Technical Paper and FYP Final Report										24 August 2012